

# ENGINEERING OF BIOMATERIALS

INŻYNIERIA BIOMATERIAŁÓW

JOURNAL OF POLISH SOCIETY FOR BIOMATERIALS AND FACULTY OF MATERIALS SCIENCE AND CERAMICS AGH-UST

CZASOPISMO POLSKIEGO STOWARZYSZENIA BIOMATERIAŁÓW I WYDZIAŁU INŻYNIERII MATERIAŁOWEJ I CERAMIKI AGH

**Number 152**

Numer 152

**Volume XXII**

Rok XXII

**OCTOBER 2019**

PAŹDZIERNIK 2019

**ISSN 1429-7248**

**PUBLISHER:**

WYDAWCA:

**Polish Society  
for Biomaterials  
in Krakow**

Polskie  
Stowarzyszenie  
Biomateriałów  
w Krakowie

**EDITORIAL  
COMMITTEE:**

KOMITET

REDAKCYJNY:

**Editor-in-Chief**

Redaktor naczelny

**Jan Chłopek**

**Editor**

Redaktor

**Elżbieta Pamuła**

**Secretary of editorial**

Sekretarz redakcji

**Design**

Projekt

**Katarzyna Trała**

**ADDRESS OF  
EDITORIAL OFFICE:**

ADRES REDAKCJI:

**AGH-UST**

30/A3, Mickiewicz Av.

30-059 Krakow, Poland

Akademia

Górnictwo-Hutnicza

al. Mickiewicza 30/A-3

30-059 Kraków

**Issue: 250 copies**

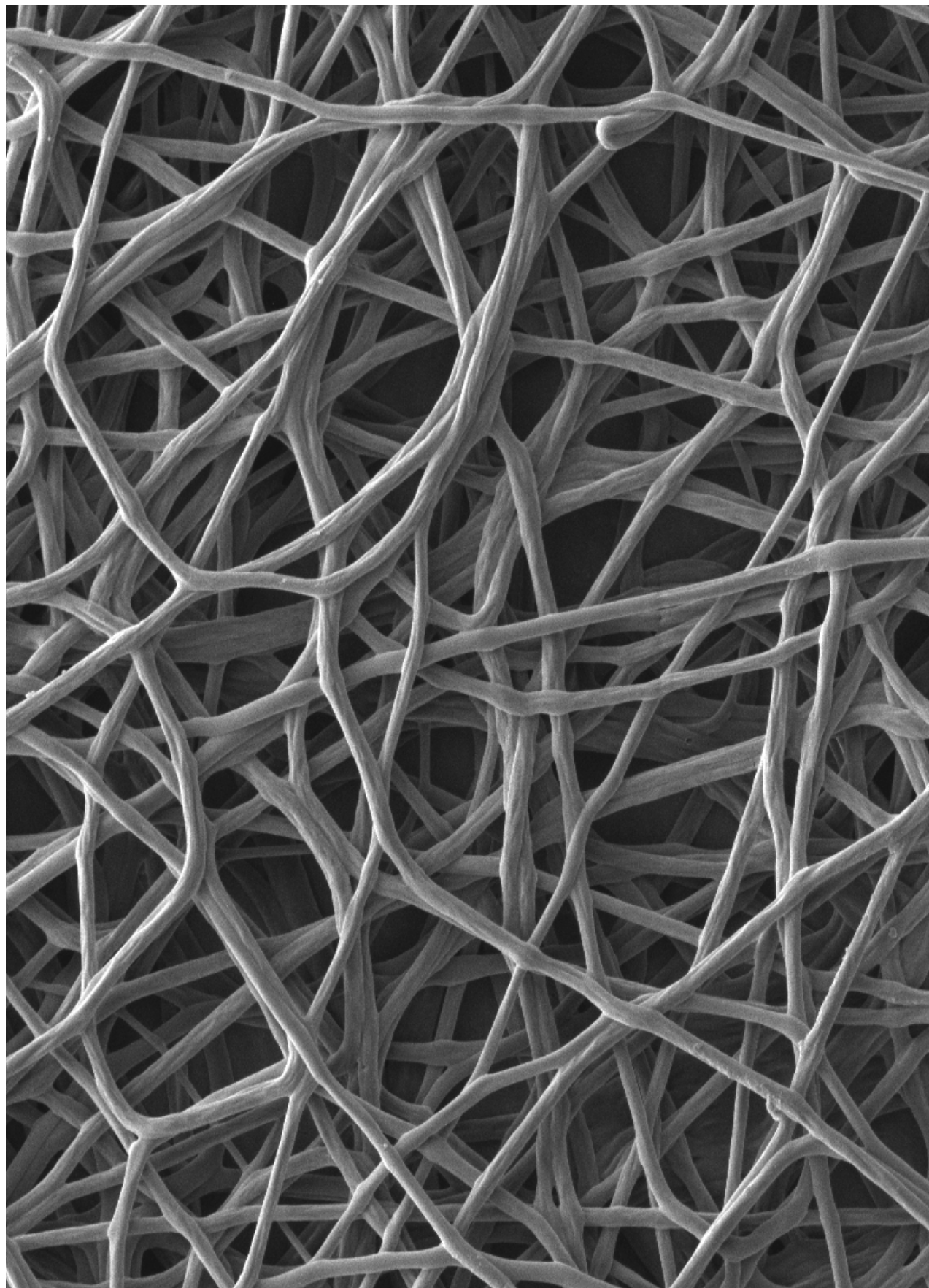
Nakład: 250 egz.

**Scientific Publishing  
House AKAPIT**

Wydawnictwo Naukowe

AKAPIT

e-mail: [wn@akapit.krakow.pl](mailto:wn@akapit.krakow.pl)



**EDITORIAL BOARD  
KOMITET REDAKCYJNY**

**EDITOR-IN-CHIEF**

Jan Chłopek - AGH UNIVERSITY OF SCIENCE AND TECHNOLOGY, KRAKOW, POLAND

**EDITOR**

Elżbieta Pamuła - AGH UNIVERSITY OF SCIENCE AND TECHNOLOGY, KRAKOW, POLAND

**INTERNATIONAL EDITORIAL BOARD  
MIĘDZYNARODOWY KOMITET REDAKCYJNY**

Iulian Antoniac - UNIVERSITY POLITEHNICA OF BUCHAREST, ROMANIA

Lucie Bacakova - ACADEMY OF SCIENCE OF THE CZECH REPUBLIC, PRAGUE, CZECH REPUBLIC

Romuald Będziński - UNIVERSITY OF ZIELONA GÓRA, POLAND

Marta Błażewicz - AGH UNIVERSITY OF SCIENCE AND TECHNOLOGY, KRAKOW, POLAND

Stanisław Błażewicz - AGH UNIVERSITY OF SCIENCE AND TECHNOLOGY, KRAKOW, POLAND

Maria Borczuch-Łączka - AGH UNIVERSITY OF SCIENCE AND TECHNOLOGY, KRAKOW, POLAND

Wojciech Chrzanowski - UNIVERSITY OF SYDNEY, AUSTRALIA

Jan Ryszard Dąbrowski - BIAŁYSTOK TECHNICAL UNIVERSITY, POLAND

Timothy Douglas - LANCASTER UNIVERSITY, UNITED KINGDOM

Christine Dupont-Gillain - UNIVERSITÉ CATHOLIQUE DE LOUVAIN, BELGIUM

Matthias Epple - UNIVERSITY OF DUISBURG-ESSEN, GERMANY

Robert Hurt - BROWN UNIVERSITY, PROVIDENCE, USA

James Kirkpatrick - JOHANNES GUTENBERG UNIVERSITY, MAINZ, GERMANY

Ireneusz Kotela - CENTRAL CLINICAL HOSPITAL OF THE MINISTRY OF THE INTERIOR AND ADMINISTR. IN WARSAW, POLAND

Małgorzata Lewandowska-Szumieł - MEDICAL UNIVERSITY OF WARSAW, POLAND

Jan Marciniak - SILESIA UNIVERSITY OF TECHNOLOGY, ZABRZE, POLAND

Ion N. Mihailescu - NATIONAL INSTITUTE FOR LASER, PLASMA AND RADIATION PHYSICS, BUCHAREST, ROMANIA

Sergey Mikhalovsky - UNIVERSITY OF BRIGHTON, UNITED KINGDOM

Stanisław Mitura - TECHNICAL UNIVERSITY OF LIBEREC, CZECH REPUBLIC

Piotr Niedzielski - TECHNICAL UNIVERSITY OF LODZ, POLAND

Abhay Pandit - NATIONAL UNIVERSITY OF IRELAND, GALWAY, IRELAND

Stanisław Pielka - WROCLAW MEDICAL UNIVERSITY, POLAND

Vehid Salih - UCL EASTMAN DENTAL INSTITUTE, LONDON, UNITED KINGDOM

Jacek Składzień - JAGIELLONIAN UNIVERSITY, COLLEGIUM MEDICUM, KRAKOW, POLAND

Andrei V. Stanishevsky - UNIVERSITY OF ALABAMA AT BIRMINGHAM, USA

Anna Ślósarczyk - AGH UNIVERSITY OF SCIENCE AND TECHNOLOGY, KRAKOW, POLAND

Tadeusz Trzaska - UNIVERSITY SCHOOL OF PHYSICAL EDUCATION, POZNAŃ, POLAND

Dimitris Tsipas - ARISTOTLE UNIVERSITY OF THESSALONIKI, GREECE

## Wskazówki dla autorów

1. Prace do opublikowania w kwartalniku „Engineering of Biomaterials / Inżynieria Biomateriałów” przyjmowane będą wyłącznie w języku angielskim.

2. Wszystkie nadsyłane artykuły są recenzowane.

3. Materiały do druku prosimy przysyłać na adres e-mail: kabe@agh.edu.pl.

4. Struktura artykułu:

• TYTUŁ • Autorzy i instytucje • Streszczenie (200-250 słów) • Słowa kluczowe (4-6) • Wprowadzenie • Materiały i metody • Wyniki i dyskusja • Wnioski • Podziękowania • Piśmiennictwo

5. Autorzy przesyłają pełną wersję artykułu, łącznie z ilustracjami, tabelami, podpisami i literaturą w jednym pliku. Artykuł w tej formie przesyłany jest do recenzentów. Dodatkowo autorzy proszeni są o przesłanie materiałów ilustracyjnych (rysunki, schematy, fotografie, wykresy) w oddzielnych plikach (format np. .jpg, .gif, .tiff, .bmp). Rozdzielczość rysunków min. 300 dpi. Wszystkie rysunki i wykresy powinny być czarno-białe lub w odcieniach szarości i ponumerowane cyframi arabskimi. W tekście należy umieścić odnośniki do rysunków i tabel. W przypadku artykułów dwujęzycznych w tabelach i na wykresach należy umieścić opisy polskie i angielskie.

6. Na końcu artykułu należy podać wykaz piśmiennictwa w kolejności cytowania w tekście i kolejno ponumerowany.

7. Redakcja zastrzega sobie prawo wprowadzenia do opracowań autorskich zmian terminologicznych, poprawek redakcyjnych, stylistycznych, w celu dostosowania artykułu do norm przyjętych w naszym czasopiśmie. Zmiany i uzupełnienia merytoryczne będą dokonywane w uzgodnieniu z autorem.

8. Opinia lub uwagi recenzentów będą przekazywane Autorowi do ustosunkowania się. Nie dostarczenie poprawionego artykułu w terminie oznacza rezygnację Autora z publikacji pracy w naszym czasopiśmie.

9. Za publikację artykułów redakcja nie płaci honorarium autorskiego.

10. Adres redakcji:

Czasopismo

„Engineering of Biomaterials / Inżynieria Biomateriałów”

Akademia Górniczo-Hutnicza im. St. Staszica

Wydział Inżynierii Materiałowej i Ceramiki

al. Mickiewicza 30/A-3, 30-059 Kraków

tel. (48) 12 617 25 03, 12 617 25 61

tel./fax: (48) 12 617 45 41

e-mail: chlopek@agh.edu.pl, kabe@agh.edu.pl

Szczegółowe informacje dotyczące przygotowania manuskryptu oraz procedury recenzowania dostępne są na stronie internetowej czasopisma:

[www.biomat.krakow.pl](http://www.biomat.krakow.pl)

## Warunki prenumeraty

Zamówienie na prenumeratę prosimy przysyłać na adres: mgr inż. Augustyn Powroźnik

apowroz@agh.edu.pl, tel/fax: (48) 12 617 45 41

Cena pojedynczego numeru wynosi 20 PLN

Konto: Polskie Stowarzyszenie Biomateriałów

30-059 Kraków, al. Mickiewicza 30/A-3

ING Bank Śląski S.A. O/Kraków

nr rachunku 63 1050 1445 1000 0012 0085 6001

Prenumerata obejmuje 4 numery regularne i nie obejmuje numeru specjalnego (materiały konferencyjne).

## Instructions for authors

1. Papers for publication in quarterly journal „Engineering of Biomaterials / Inżynieria Biomateriałów” should be written in English.

2. All articles are reviewed.

3. Manuscripts should be submitted to editorial office by e-mail to kabe@agh.edu.pl.

4. A manuscript should be organized in the following order:

• TITLE • Authors and affiliations • Abstract (200-250 words) • Keywords (4-6) • Introduction • Materials and Methods • Results and Discussions • Conclusions • Acknowledgements • References

5. All illustrations, figures, tables, graphs etc. preferably in black and white or grey scale should be additionally sent as separate electronic files (format .jpg, .gif, .tiff, .bmp). High-resolution figures are required for publication, at least 300 dpi. All figures must be numbered in the order in which they appear in the paper and captioned below. They should be referenced in the text. The captions of all figures should be submitted on a separate sheet.

6. References should be listed at the end of the article. Number the references consecutively in the order in which they are first mentioned in the text.

7. The Editors reserve the right to improve manuscripts on grammar and style and to modify the manuscripts to fit in with the style of the journal. If extensive alterations are required, the manuscript will be returned to the authors for revision.

8. Opinion or notes of reviewers will be transferred to the author. If the corrected article will not be supplied on time, it means that the author has resigned from publication of work in our journal.

9. Editorial does not pay author honorarium for publication of article.

10. Address of editorial office:

Journal

„Engineering of Biomaterials / Inżynieria Biomateriałów”

AGH University of Science and Technology

Faculty of Materials Science and Ceramics

30/A-3, Mickiewicz Av., 30-059 Krakow, Poland

tel. (48) 12) 617 25 03, 12 617 25 61

tel./fax: (48) 12 617 45 41

e-mail: chlopek@agh.edu.pl, kabe@agh.edu.pl

Detailed information concerning manuscript preparation and review process are available at the journal's website:

[www.biomat.krakow.pl](http://www.biomat.krakow.pl)

## Subscription terms

Contact:

MSc Augustyn Powroźnik,

e-mail: apowroz@agh.edu.pl

Subscription rates:

Cost of one number: 20 PLN

Payment should be made to:

Polish Society for Biomaterials

30/A3, Mickiewicz Av.

30-059 Krakow, Poland

ING Bank Śląski S.A.

account no. 63 1050 1445 1000 0012 0085 6001

Subscription includes 4 issues and does not include special issue (conference materials).







# 29<sup>th</sup> Biomaterials in Medicine and Veterinary Medicine Annual Conference

15 – 18 October 2020 Rytro, Poland

SAVE THE DATE

15-18

OCTOBER  
2020

[www.biomat.agh.edu.pl](http://www.biomat.agh.edu.pl)






REGISTER  
AND  
SUBMIT  
AN ABSTRACT



## **SPIS TREŚCI CONTENTS**

<b>NANOTECHNOLOGY IN ONCOLOGY - CURRENT STATE OF KNOWLEDGE</b> DOROTA LASKOWSKA, EWA ZIÓŁKOWSKA, KATARZYNA MITURA	<b>2</b>
<b>SYNTHETIC EXTRACELLULAR MATRIX AS A SUBSTRATE FOR REGENERATIVE MEDICINE</b> EWA STODOLAK-ZYCH, ELŻBIETA MENASZEK, ALEKSANDRA TWARDY, ANNA ŚCISŁOWSKA- CZARNECKA, MACIEJ BOGUŃ, BEATA KOLESIŃSKA	<b>10</b>
<b>DEVELOPMENT OF A NEW PRODUCTION METHOD OF FOAM-LIKE WOUND DRESSINGS FOR SKIN REGENERATION</b> VLADYSLAV VIVCHARENKO, PAULINA KAZIMIERCZAK, MICHAŁ WÓJCIK, AGATA PRZEKORA	<b>16</b>
<b>WPŁYW WARSTWY POŚREDNIEJ NA POŁĄCZENIE METAL-CERAMIKA INFLUENCE OF THE INTER-MEDIATE LAYER ON THE METAL-CERAMICS BOND STRENGTH</b> ZOFIA KULA, ŁUKASZ KOŁODZIEJCZYK, HIERONIM SZYMANOWSKI	<b>21</b>

# NANOTECHNOLOGY IN ONCOLOGY - CURRENT STATE OF KNOWLEDGE

DOROTA ŁASKOWSKA<sup>1\*</sup> , EWA ZIÓŁKOWSKA<sup>1</sup> ,  
KATARZYNA MITURA<sup>2</sup> 

<sup>1</sup> THE PRESIDENT STANISŁAW WOJCIECHOWSKI STATE  
UNIVERSITY OF APPLIED SCIENCES IN KALISZ,  
NOWY ŚWIAT 4, 62-800 KALISZ, POLAND

<sup>2</sup> KOSZALIN UNIVERSITY OF TECHNOLOGY,  
ŚNIADECKICH 2, 75-453 KOSZALIN, POLAND

\*E-MAIL: DOROTA.LASKOWSKAPL@GMAIL.COM

## Abstract

*Nanotechnology is an interdisciplinary area of science devoted to the production and testing of nanostructures - defined as forms of the matter organizations the size of which does not exceed 100 nm. It is a quickly developing area of science with many applications in different areas of life, for example in engineering, computing, medicine, pharmacy, and agriculture.*

*One of the problems of contemporary oncology is the low specificity of applied therapies. Most currently used chemiopharmaceuticals have systemic effects which not only affect cancer cells but also healthy tissues. Complications after chemotherapy observed in many patients are bone marrow deficiency (neutropenia, thrombocytopenia, anemia), damage to the nervous system (neurotoxicity), myocardium (cardiotoxicity) and pulmonary parenchyma. Similarly, in radiotherapy, ionizing radiation destroys the healthy tissues in the irradiation field. The side effects of radiation therapy may include fatigue, skin reactions, and impairment of tissue and organ functions. According to studies, nanostructures are an opportunity to overcome these limitations. The most popular nanostructures used in medicine are liposomes, silver and gold nanoparticles, magnetic nanoparticles, carbon nanotubes, and dendrimers.*

*The purpose of this article is to present the current state of knowledge on the use of available nanotechnology solutions in pharmacology and cancer treatment.*

**Keywords:** nanotechnology, oncology, nanostructures, cancer treatment

*[Engineering of Biomaterials 152 (2019) 2-9]*

## Introduction

Richard Feynman, the visionary of developing nanotechnology as a separate branch of science, as early as 1959, predicted the possibility of precise manipulation and controlling the position of atoms in material structures. The first attempt to define this concept was made in 1974 by Nobuteru Taniguchi. He based his considerations on the dimensional criterion and referred (similarly to R. Feynman) to the possibility of designing materials at the nanoscale. However, at that time this was only a theory limited by the available resolution capabilities of the microscopes [1,2].

A significant step forward was the development of the scanning tunneling microscope (STM) in 1981 and the atomic force microscope (AFM) in 1982. Since then, these tools have made it possible to observe the materials surface with the single-atom resolution [1,2].

The new tools led to new discoveries. In 1985, Richard Smalley, Harold Kroto, and Robert Curl discovered a new allotropic form of carbon-fullerenes. Inspired by their research, in 1991 Sumio Iijima discovered carbon nanotubes: structures characterized by high thermal conductivity and unique mechanical and electrical properties. These discoveries were the starting point for future research, the purpose of which was not only to develop technologies to produce nanostructures and nanomaterials but also to enhance them with specific biological properties, particularly for future applications in medicine, pharmacy, and cosmetology [1,2].

## Methods of production and division of nanostructures

The term "a nanostructure" is defined as the natural or artificial form of the organization of matter in a condensed and isolated form, made up of atoms, particles or clusters, whose dimensions are limited to nanoscales (where the size does not exceed 100 nm). The material built on a media using nanostructures is called a nanomaterial. Sometimes in literature, the interchangeable use of these terms occurs [1,2].

The reduction of matter to the nanoscale can take place in one of three dimensions (in the coordinate system). Based on this principle, nanostructures are divided into zero, one, two and three-dimensional ones [3].

There are many methods employed to obtain artificial nanostructures which can be divided into three general groups:

- top-down methods which consist in the comminution of macroscopic materials (obtained by traditional methods) into smaller parts, using physical processes,
- bottom-up methods which consist in the controlled production of larger material structures by combining and moving single atoms and molecules, using chemical processes,
- hybrid methods [1,3,4].

Regardless of the production method, nanostructures obtained have interesting properties which are different when compared to the properties of micro- and macrometric materials.

## Nanomedicine

Of all the applications of nanostructures and nanomaterials in medicine those which deserve special attention are:

- pharmacy, in particular the search for new antibacterial, antiviral or antifungal agents and carriers of drug and biological molecules,
- nanooncology which includes different activities to improve existing treatment methods and to develop new alternative therapies, notably targeted therapy, photodynamic therapy or thermotherapy,
- diagnostic and medical equipment, including the use of nanostructures as biosensors and contrast agents,
- regenerative medicine, implantology, and dentistry.

Regarding cancer diagnosis and therapy, the use of multifunctional nanoparticles called theranostic systems are a promising prospect [5].



### Antiseptic agents and materials

Bacteria have accompanied humanity since the very beginning. They can be found not only in soil and water but also in extreme environments, such as glaciers or hydrothermal waters. Moreover, they can survive in both aerobic and anaerobic conditions. Along with the development of microbiology, at the turn of the 19<sup>th</sup> and 20<sup>th</sup> centuries, there was a breakthrough for medicine) as researchers confirmed the existence of pathogenic bacteria. Initially, precious metal compounds, including silver and gold, were used to combat bacteria.

In the 19<sup>th</sup> century, silver compounds were widely used to treat infections associated with ulceration, burns or wounds which were difficult to heal and to treat diseases, such as epididymitis, tonsillitis or conjunctivitis. In 1928 the first antibiotic – penicillin, was discovered. Currently, antibiotics are in common use. However, the increasing overuse and also misuse of antibiotics resulted in the spread of drug-resistant bacterial strains. Considering the scale and seriousness of the problem, the research on alternative antibacterial agents, including nanostructures, has started [6,7].

According to studies, silver nanoparticles display particular bactericidal potential. Nanoparticles are nanostructures created by reducing the initial material (in macro-scale) in all three dimensions so that all the dimensions measure below 100 nm. Nanoparticles have unique physico-chemical properties when compared to the materials with the same chemical composition but at the macro scale, due to the significant ratio of their surface atoms to the core atoms [1,2,8].

The impact of silver nanoparticles on biological systems consists in breaking up cell membranes, denaturing proteins, disrupting and inhibiting DNA replication, producing oxygen radicals and the expression of proteins and enzymes in the respiratory chain. Their effectiveness depends, among other factors, on the size and shape of the applied nanoparticles, the type of bacteria (cell wall structure) and the environment (the presence of oxygen, pH or temperature) [6,8].

In many studies, the toxic effects of nanosilver have been confirmed against such bacteria as: *Staphylococcus aureus* (which causes purulent skin infections, subcutaneous and soft tissue infections, systemic infections and toxic shock syndrome associated with the production of toxins), *Escherichia coli* (which causes food poisoning, urinary tract infections, neonatal meningitis, organ abscesses, sepsis), *Pseudomonas aeruginosa* (particularly common in patients with cystic fibrosis), *Chlamydia trachomatis* (which transmitted during sexual interaction causes a disease called chlamydia) and *Providencia stuartii* (which occurs in patients with severe burns or long-term urinary catheters) [8,9].

The aforementioned bacteria are the most common sources of nosocomial infections which are especially dangerous for oncological patients. Patients undergoing radiotherapy suffer from the immunity decrease related to the impaired hematopoietic system (bone marrow) due to the ionizing radiation. Cytostatics and immunosuppressants have a similar effect. In general, the general destruction of the body is associated with the ongoing process of cancer and its treatment. To protect the weakened patients against bacterial infections, silver nanoparticles are used in the production of bandages, surgical masks, catheters, implants, and medical equipment. Apart from medical applications, nanosilver is also introduced into building materials (e.g. paints), home water treatment plants, textiles, and household items, which are interesting areas for further research as well [1,6,8,9].

### Nanostructures as drug carriers in targeted therapy

The main purpose of any cancer therapy is to destroy as many cancer cells as possible while protecting healthy tissue and minimizing potential complications. As years of experience show, this goal is not always easy and achievable. Therefore, it is hoped that the targeted therapy using nanostructures as carriers of therapeutic compounds will help to eliminate the adverse effects of treatment.

Due to the unique properties of nanostructures, they can penetrate through the cells membrane (including overcoming the blood-brain barrier), increase the half-life and specificity of the active substance and delay the drug metabolism. Drug delivery systems affect the stability, biodistribution, and solubility of the provided medicament which is released directly at the site of the disease. Thus, the active substance is accumulated in the cells or tissue where most needed. The drug-carrier combination is called a conjugate [10,11].

Regarding the mechanism, the targeted therapy is divided into:

- passive therapy (FIG. 1) using the phenomenon of the increased permeability of blood vessels which supply nutrients to the cancer cells. The nanoparticles contained within the drug freely penetrate the cell or get absorbed via endocytosis. This effect of increased permeability and retention (EPR effect) of nanostructures in cancer cells concerns mainly the nanoparticles systems similar to micellar systems, liposomes, polymeric-drug conjugates and polymeric NPs [10,12-14].
- active therapy (FIG. 2) using a combination of nanoparticle, drug, and ligand. The ligand is usually a substance with a strong affinity for tumour cell membrane receptors or a compound these cells demand for e.g. glucose or folic acid [10,12-14].

Nanoparticles with magnetic properties also serve as efficient carriers. In such cases, the conjugate will stop at the target site when the magnetic field is stronger than the linear blood flow [10].

The nanostructures used as drug carriers have to meet a number of requirements concerning biocompatibility, non-toxicity and limited accumulation in the body, as nanoparticles are absorbed and degraded in the liver or spleen. The active functional groups should be located on the surface to maintain the therapeutic properties. Sometimes, in order to fulfill the strict requirements, it is necessary to functionalize nanostructures [10,15,16].

The most popular modification involves the use of polymers, such as polyethylene glycol (PEG), N-(2-hydroxypropyl)methacrylamide copolymer (HPMA), a polystyrene copolymer with maleic anhydride, poly(L-glutamic acid (PG) and poly (D,L-lactic-co-glycolic acid (PLGA). Of those listed, the most commonly used is PEG, due to its high solubility in water, biodegradability, minimal toxicity and controlled mechanical properties [17,18]. The functionalization process can also involve applying proteins and sugars [10].

Nanostructures that can be used as drug carriers in oncology are, among others, liposomes, gold nanoparticles, carbon nanotubes, and dendrimers.

Liposomes are nanoparticles of colloidal spherical-shaped structures. They are composed of a double lipid layer surrounding a central water space where the drug or other active substance is placed. As research shows, the release of the drug from the conjugate results from the liposome decay caused by the low pH of the tumour microenvironment. To prolong the circulation time in the body and improve the targeted drug delivery, the liposomes are coated with polyethylene glycol chains (PEGylated liposomes) [10,12,14].



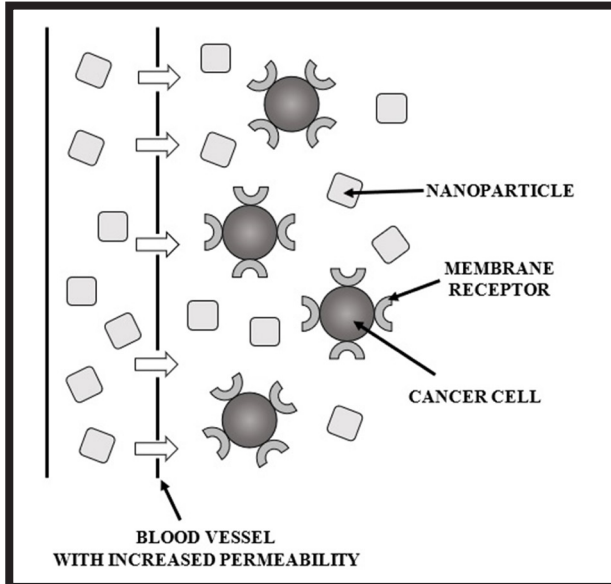


FIG. 1. The passive targeted therapy mechanism, based on Bitulicki (2016) [13].

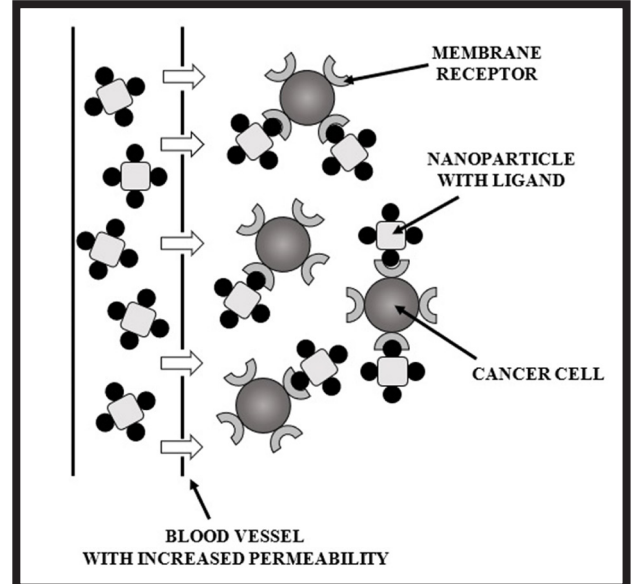


FIG. 2. The active target therapy mechanism, based on Bitulicki (2016) [13].

TABLE 1. Nanoparticles based drug approved by FDA, based on Raj (2019) [14].

Name	Nanotechnology platform	Active pharmaceutical ingredient	Cancer type
DepoCyt	Liposome	Cytarabin	HIV-related Kaposi sarcoma
DaunoXome	Liposome	Duanotubicin	HIV-related Kaposi sarcoma
Myocet	Liposome	Doxorubicin	Metastatic breast cancer
Marqibo	Liposome	Vincristine Sulfate	Acute lymphoblastic leukemia
Mepact	Liposome	Muramyl tripeptide phosphatidylethanolamine	Nonmetastatic, resectable osteosarcoma
Onivyde	Liposome	Irinotecan	Pancreatic cancer
Doxil	PEGylated liposome	Doxorubicin	HIV-related Kaposi sarcoma, ovarian cancer, multiple myeloma
Onivyde/MM-398	PEGylated liposome	Irinotecan	Post-gemcitabine metastatic pancreatic cancer
Abraxane	Albumin NP	Paclitaxel	Breast, lung and pancreatic cancer
Genexol-PM	Polymeric micelle	Paclitaxel	Breast cancer and non-small-cell lung carcinoma (NSCLC)
Oncaspar	Polymer protein conjugate	L-asoaraginase	Leukemia
NanoTherm	Iron oxide NP		Thermal ablation glioblastoma

The liposomes functionalized with polyethylene glycol (PEG) are used as a carrier of doxorubicin. The research has shown the increased conjugate accumulation at the cancer site in comparison to the unbound drug. This phenomenon facilitates the effectiveness of the therapy while reducing the side effects. This conjugate was approved by the Food and Drug Administration for the treatment of breast cancer, ovarian cancer, multiple myeloma and Kaposi's sarcoma [10,12,19].

The first nanotechnology-based drugs with tFDA approval are Abraxane and Doxil. TABLE 1 presents nanoparticles-based drugs approved by FDA for different types of cancer treatment.

Gold nanoparticles (GNPs) are stable and non-toxic and their proper functionalization allows for the attachment of various active substances [18]. Studies have proved GNPs as an effective carrier for such chemopharmaceuticals as oxaliplatin (a derivative of cisplatin) used to treat colorectal cancer. Oxaliplatin is characterized by high neurotoxicity and a negative impact on the patient's well-being (nausea and vomiting), which significantly limits its applications. In order to reduce its harmfulness, oxaliplatin is combined with gold nanoparticles modified by polyethylene glycol (PEG-GNPs). The results of the studies revealed that such a conjugate is six times more efficient than the drug in an unbound form [11].

Carbon nanotubes (CNTs) are nanometric structures shaped as empty cylinders built of coiled graphene planes. Such a structure provides CNTs with numerous unique optical, chemical, physical and mechanical properties. The carbon nanotubes come in a variety of structures either single-walled (composed of single graphene layers) or multi-walled (containing many concentrically arranged graphene cylinders). In order to use nanotubes as drug carriers, they must be functionalized [20,21].

The first use of nanotubes as drug carriers (*in vivo*) was documented in 2008 by Z. Liu [22]. In the studies, paclitaxel was attached to the single-walled carbon nanotubes (previously modified by polyethylene glycol with an amino moiety). This system was characterized by great solubility, the long residence time in the blood circulation and better uptake by tumour cells, which contributed to the high drug accumulation in the tumour area. Moreover, the tumour resorption was observed after the application of even small amounts of the conjugate [12,23].

In the following years, the researchers studied nanotubes as transport systems for such compounds as:

- cisplatin [14,19-25]

Particular attention should be paid to the works of C. Tripisciano et al. [24,25] who presented a method of introducing cisplatin (DDP) into the structure of single-walled (SWCNTs) and multiwalled (MWCNTs) carbon nanotubes. The researchers analyzed the effects of various drug concentrations both in an unbound form and the conjugate on the cells viability (prostate cancer). They observed a direct proportional dependence of the increase in the SWCNTs-DDP conjugate content on the cancer destruction. Although the effectiveness of SWCNTs-DDP and the unbound drug was comparable, the conjugate caused fewer side effects. Interesting results (TABLE 2) were obtained by comparing two types of carriers with regard to the drug transfer efficiency.

Although the method of introducing cisplatin in both cases was the same, the amount of drug accumulated in MWCNTs was lower than in SWCNTs. In addition, the MWCNTs-DDP conjugate was characterized by higher efficiency and speed of drug release. The researchers associated this fact with the lack of mutual interactions in the cisplatin-MWCNTs system [17,23].

- carboplatin [17,23,22]

The work in this area was conducted, among others, by the S. Hampel research group [26]. According to the research results, the carboplatin-CNTs conjugate significantly slowed the growth of cancer cells in the blood [17,23].

- doxorubicin [23,27]

H. Ali-Boucetta and his research group [27] used the doxorubicin combined (non-covalent bond) with multi-walled carbon nanotubes (previously modified with the triblock copolymer). This combination contributed to the better drug delivery to the diseased cells (breast cancer) through biological barriers and it improved the drug activity. In addition, the conjugate system increased drug toxicity against breast cancer cells [23].

Despite the potential benefits, the use of nanotubes as drug carriers is often questioned because of toxicity concerns. Nevertheless, the research by J. Yan et al. [28] showed that the injection of carbon nanotubes into tissues around the tumour did not cause any side effects [14,29].

Dendrimers are complex, highly branched polymers composed of a multifunctional centre (core) and arms called dendrons. Free functional groups, located at the end of dendrons, can be modified in order to change chemical and physical properties of the molecule. Dendrimers are characterized by free spaces called cavities that can encapsulate various compounds, such as drugs and biologically active molecules. There are many types of dendrimers, including polyamidoamine (PAMAM), poly(propylene imine) (PPI), polyether or carbosilane (DBD) [1,8,30,31].

The researchers considered utilizing dendrimers as transport systems for such compounds as:

- methotrexene [8,31]

In studies performed on mice with a subcutaneous tumour of human epidermal carcinoma, PAMAM dendrimers (5<sup>th</sup> generation) were used. The modification consisted in folic acid (ligand), fluorescein (fluorophore) and methotrexene attachment to the acetylated surface functional groups. Following the conjugate intravenous administration, the researchers observed the increased drug accumulation in the tumour cells with overexpressing folic acid receptors and the significant inhibition of the tumour growth [8,31].

- cisplatin [12,30,31]

The conjugate of cisplatin and PAMAM dendrimers proved the increased drug accumulation in the tumour and its retarded release. This translated into weaker toxicity as compared to the therapy with cisplatin alone [12,30,31].

- doxorubicin [12,31]

In research on human gingiva tumour line cells (Ca9-22 cells), the researchers compared two different conjugates of PAMAM dendrimers and doxorubicin (DOX). The results showed the superiority of the hydrazone coagulate (PAMAM-hyd-DOX) over the amido coagulate (PAMAM-amide-DOX). The PAMAM-hyd-DOX conjugate disintegrated in the acidic environment, releasing the drug which led to the tumour cells death. The conjugate cytotoxicity against the tumour cells may have increased due to so-called chemical internalization [12,31].

- 5-fluorouracil (5FU) [31],

- gemcitabine [9],

- ibuprofen (results: an increase in the drug concentration in epithelial lung cancer cells) [8,31].

TABLE 2. Effectiveness of DDP delivery by SWCNTs and MWCNTs, based on Werengowska (2012) [17].

	SWCNTs	MWCNTs
The amount of medicine inside CNTs	21 µg/100 µg CNTs	13.6 µg/100 µg CNTs
The amount of drug released	68%	95%
The rate of drug release	Slower	Faster
Time to release the maximum dose	72 h	48 h

In light of the above considerations, the targeted therapy using nanostructures as drug carriers is a promising alternative to traditional chemotherapy. The described solutions allow to eliminate such problems as low efficiency in drug distribution, low bioavailability, increasing resistance of tumour cells to cytostatics and the high systemic toxicity of therapy [12]. TABLE 3 summarizes the conjugates which were described above.

**TABLE 3. Nanostructures used as drug carriers - exemplary applications.**

Nanostructures	Active substance	Literature
Liposomes	Doxorubicin	[10, 12]
Gold nanoparticles (GNPs)	Oxaliplatin	[11]
Carbon nanotubes (CNTs)	Paclitaxel	[12, 22, 23]
	Cisplatin	[17, 23-25]
	Carboplatin	[17, 23, 26]
	Doxorubicin	[23, 27]
Dendrimers	Methotrexene	[8, 31]
	Cisplatin	[12, 30, 31]
	Doxorubicin	[12, 31]
	5-fluorouracil (5FU)	[31]
	Gemcitabine	[9]
	Ibuprofen	[8, 31]

#### Photodynamic therapy

Another alternative to traditional chemotherapy is photodynamic therapy. It involves the application of a photosensitizing agent activated by the electromagnetic radiation of a specific wavelength which corresponds to the absorption band of the sensitizer. Thus reactive oxygen species (mainly singlet oxygen) are released, which leads to the microcirculation damage and induces the local inflammatory reaction resulting in the tumour cells death. The commonly used photosensitizers are orally administered compounds which accumulate not only in the tumour area but also in other tissues. The particularly vulnerable organs are the eyes and skin, due to their substantial exposure to sunlight [12,13,32].

Nanostructures in the photodynamic therapy (similar to the targeted therapy) are used to produce conjugates providing photosensitizers directly to the tumour. In this regard, once again, the usefulness of such nanostructures as carbon nanotubes and dendrimers has been confirmed [12].

The research group of V.N. Khabashsek [33] tested a complex of folic acid (ligand), carbon nanotubes and a photosensitizer from the porphyrin group. After the conjugate administration, its high affinity for the tumour cells was confirmed by the highest drug concentration in this area. In the next step, their radiation using a laser of the appropriate wavelength initiated the process of producing singlet oxygen. The therapy effectiveness depended on the malignancy degree of the neoplastic lesion, with better results obtained against malignant tumours. Still, the therapy effectiveness was not lower than 60% [20,33].

#### Thermotherapy

Another promising strategy for cancer treatment is thermotherapy which uses the stimulating and destructive effects of thermal energy on the cellular structures. An increase in the body temperature may have internal (endogenous) or external (exogenous) causes. Depending on the purpose, there are two types of thermotherapy:

- hyperthermia when the temperature increase to 42-46°C is aimed at sensitizing tissue to the traditional therapy (chemotherapy or radiotherapy),
- thermoablation when the temperature increase to 51-55°C leads to cell death [12].

The most basic classification of hyperthermia methods refers to the size of the body area subjected to high temperatures. Therefore, one can distinguish the local, regional and systemic (whole-body) hyperthermia. The classification shown in TABLE 4 additionally takes into account the tumour location [34].

**TABLE 4. Different types of hyperthermia - exemplary classification, based on Rzepka (2012) [34].**

Local hyperthermia	Regional hyperthermia	Whole-body hyperthermia
External methods - applicators on the body surface	Treatment of deep tissue cancers	
Intraluminal or endocavitary methods - applicators inside the body cavities	Regional perfusion techniques	
Interstitial methods (including thermoablation)	Continuous hyperthermic peritoneal perfusion (CHPP)	

In oncology, hyperthermia is defined as a controlled technique of heating the cancer area in order to destroy the tumour cells or inhibit their growth [34]. Pathological tissues with disturbed thermoregulation processes are not able to effectively discharge the heat excess, which leads to denaturation of the protein structures and the cell death [13].

Hyperthermia has its limitations. In the case of advanced pathological changes, it is difficult to introduce the applicator and in the case of small changes and the micrometastases the precise location is problematic. Moreover, the side effect of overheating healthy tissues may damage them. The safe temperature limit is about 44°C with the exposure time of about 60 minutes. However, it is difficult to maintain the steady temperature all over the heated area, especially during the intraluminal or endocavitary hyperthermia. Additionally, some tissues are more sensitive to heating and this factor should be taken into account as well. Most disadvantageous side effects occur during whole-body hyperthermia, including diarrhea, nausea, vomiting, skin burns, heart problems and changes in the coagulation system. That is why, in contemporary oncology, hyperthermia is used mainly to accompany radio- and chemotherapy. In order to eliminate the drawbacks of thermotherapy the possibility of using nanotechnology and nanostructures was studied [3,12,13,34].



The nanostructures that can be used in thermotherapy are, among others, gold nanoparticles and supermagnetic iron oxide nanoparticles. Gold nanoparticles are able to convert near-infrared electromagnetic radiation into heat energy. The properly functionalized GNPs accumulate in cancer cells, which allows to localize the lesions of various advancement stages and micrometastases. Thus, it is possible to heat the tumour area to the temperature of about 50°C, while protecting the healthy tissues. The increased absorption of the infrared radiation by gold nanoparticles is accompanied by the minimal radiation absorption in the case of healthy tissues [8,34,35].

The works of D.V. Peralta's research team [36] focused on the efficiency of a complex of gold nanoparticles (in the form of nanowires, AuNRs), the human serum albumin (HSA) and paclitaxel (PAC) against the mouse breast cancer cells (4T1). Having incubated the cells in the conjugate of various concentrations, the irradiation process was carried out using infrared radiation. The control group consisted of the 4T1 cells modified only with the GNPs and treated with infrared radiation. The results of the control group proved a strong dependence of the cell viability on the GNPs concentration. In turn, the IR irradiation raised the amount of paclitaxel released from the PAC-AuNR-HSA complex. Moreover, the longer the exposure time, the more drug was released from this conjugate. The most important conclusion was the synergy effect – the cells resistant to paclitaxel alone may have been killed by hyperthermia and vice versa [13,6].

Magnetic nanoparticles (MNPS) consist of an inorganic core (e.g. iron oxide, cobalt or nickel) and a shell which is compatible with specific tissues. The MNPS have different properties dependent on the composition and size of the core and the type of surface ligand. Regarding medical applications, their most important feature is superparamagnetism [8].

Superparamagnetic nanoparticles of iron oxide (SPIO) are able to generate thermal energy under the influence of an external magnetic field. This phenomenon is used in the induction heating cancer therapy (IHCT). According to the research, the necessary conditions for the effective IHCT is the temperature of 50°C maintained in the heated area for about 10 min. This therapy worked in the case of cancer foci whose size exceeds approximately 10 mm. In the smaller cancer changes (1-5 mm), the cells rapidly dissipated heat to their surroundings [12,34]. The clinical trials on the magnetic thermotherapy were conducted in several centres in Germany to treat malignant brain tumours, prostate cancer, esophageal cancer, breast cancer, rectal cancer, pancreatic cancer, bronchial cancer, cervical cancer and sarcomas [37].

The research group of Q. Zhao [38] tested the magnetic iron oxide nanoparticles inducing hyperthermia in the cases of head and neck cancer. The tests were performed using a mouse xenograft model of human head and neck squamous cell carcinoma (HNSCC) cell line (Tu212). The magnetic nanoparticles were delivered through intratumoral injection. The temperature of the tumour centre elevated quickly and the cells death occurred due to oncotic necrosis, as a consequence of hyperthermia [38].

In addition, it is possible to modify iron oxide nanoparticles by attaching therapeutic compounds to their surface, e.g. SPIO conjugates with methotrexate or doxorubicin [12]. To sum up, the application of nanotechnology in hyperthermia helps to control the temperature distribution in the tumour area and the healthy tissues exposure to heat.

Developing nanostructures with a higher radiation absorption coefficient may establish hyperthermia as an independent cancer treatment method. Nanotechnology also gives the opportunity to develop a non-invasive form of ablation [12,34]. For instance, the targeted thermal ablation of breast cancer cells using an anti-HER2 conjugated nanoparticle was tested in animal models with a positive therapeutic effect [19].

### Radiotherapy

In the course of radiotherapy, both diseased and healthy tissues in the radiation field are exposed to the harmful effects. In some cases, to protect the critical organs, it is necessary to limit the area of radiation or reduce the therapeutic dose, which may lower the therapy effectiveness.

One of the methods to improve the therapy procedures is radiosensitization. This method consists in introducing the agents, so-called radiosensitizers, that make the tumour cells more sensitive to the ionizing radiation. The ideal radiosensitizer should be:

- easily accessible,
- non-toxic under normal conditions and cytotoxic against the tumour cells when combined with certain agents,
- relatively quickly removable from the body [12,13].

The nanostructures that have been used in radiosensitization are gold nanoparticles.

W. N. Rahman's research team [39] used bovine aortic endothelial cells (BAEC) as their experimental model. It should be noted that BAECs are not cancer cells and the purpose of the research was to analyze how GNPs can facilitate the radiation dose efficiency in biological systems. In the experiment, GNPs (1.9 nm diameter) were suspended in a spherical medium at four different concentrations: 0.125, 0.25, 0.5 and 1 mM. The incubation time of the GNPs and the cells was 24 h. Before the radiation, the researchers performed:

- the optical uptake test (confocal microscopy) to observe the accumulation of gold nanoparticles clusters in the cytoplasm of the BAECs,
- the cytotoxicity test which showed the decrease in cell viability with the GNPs concentration increase.

The cell irradiation was carried out in several variants, i.e. x-rays with energies of 80 and 150 keV and electrons with energies of 6 and 12 MeV, providing different doses (0, 1, 2, 3, 4 and 5 Gy). For all types of radiation, the researchers observed a decrease in cell viability with increasing concentrations of gold nanoparticles. The highest efficiency was observed for the 80 keV X-rays in combination with the GNPs concentration of 1 mM and a dose of 4 Gy (the final cell viability was about 25%). For this combination, the dose increase factor (based on viability curves) was 24.6, as compared to 4 for the electrons with the 6 MeV energy. Therefore, it can be concluded that thanks to gold nanoparticles the megavoltage electron radiation beams were replaced with orthovoltage x-ray beams [13,39].

In other studies, F. Geng's [40] research team used human ovarian cancer cells (SK-OV-3, HTB-77) and gold nanoparticles both in an unbound form and bonded with thio-glucose (Glu-GNPs) in two concentrations: 1 and 5 nM. The incubation time of GNPs and the cells was: 1, 2, 4, 8, 12, 24, 48 and 96 h. The irradiation was performed using x-ray beams with the 80 keV and 6 MeV energies obtained from an x-ray tube and a medical linear accelerator, respectively. The total dose for all the samples was 10 Gy. The effectiveness of the three therapies: using gold nanoparticles alone, irradiation alone and GNPs combined with irradiation was analyzed.

Based on the tests, the following was found:

- higher absorption of Glu-GNPs than GNPs without modification,
- no significant harmful effects of gold nanoparticles against SK-OV-3 cells (viability at 97% in all the samples, regardless of incubation time),
- a slight, yet comparable to the control, increase in the level of apoptotic cells after incubation of GNPs,
- a lower number of cancer cells in the G0 / G1 phase (low radiation sensitivity) and a higher number of cells stopped in the G2 / M phase (high radiation sensitivity) after incubation of GNPs,
- lower cell viability for both types of radiation, with the viability rate around 45% for the orthovoltage radiation and 58% for the megavolt radiation,
- higher apoptosis induction after irradiation (e.g. for the 6 MeV energy radiation - the increase from 9.26% to 14.35%),
- the induction of oxidative stress for both types of radiation which contributed to the higher level of reactive oxygen species in the cells [13,40].

Summing up, the results revealed a better therapeutic effect of gold nanoparticles combined with radiation as compared to the irradiation alone [13,40]. The influence of gold nanoparticles on changes in the cell cycle, and therefore the increase in their radiosensitivity, was also studied by W. Roa [13,41].

There were also studies carried out by the research team of S. Setup [42] testing conjugates of gold nanoparticles and therapeutic compounds combined with irradiation. The research was to determine the therapeutic effect of the GNPs-cisplatin conjugate and the radiotherapy on the glioblastoma multiforme (one of the most aggressive malignant neoplasms). The irradiation was carried out using a source containing Caes-137 (1 Gy/min, total dose 10 Gy). The initial test results indicated that the application of the GNPs-cisplatin conjugate contributed to the decrease in the cell growth rate. The complex was cytotoxic against the tumour cells and increased the cytotoxicity of the ionizing radiation. Unfortunately, on 16<sup>th</sup> day of the experiment, the glioblastoma multiforme cells began to take reparative action [13,42].

Another area of research is the use of nanostructures as carriers of radioisotopes, e.g. yttrium <sup>90</sup>Y [12].

## Conclusions

The collected data indicates that intensive research on nanotechnology will broaden the spectrum of its applications in medicine. Thanks to their specific physicochemical properties, nanostructures will be used to improve the diagnostics, treatment, monitoring and prevention of many diseases, including cancer.




The overuse of antibiotics and bactericides has contributed to the introduction and spread of drug-resistant bacterial strains, which is a growing problem, particularly for public health institutions. A promising solution might be the use of silver nanoparticles which show toxic effects against such bacteria as *Staphylococcus aureus*, *Escherichia coli*, *Pseudomonas aeruginosa*, *Chlamydia trachomatis* or *Providencia stuartii*.

The nanostructures have also been used in the cancer treatment (nanoncology) as:

- drug carriers in the target treatment  
The nanostructures effectively used in this area are liposomes, gold nanoparticles, carbon nanotubes and dendrimers. In most cases, the use of conjugates facilitates the effectiveness of therapy or reduces its toxicity (in comparison to drugs in the unbound form). Currently, a few nanoparticles-based drugs are already approved by FDA and commercially used.
- photosensitizer carriers in the photodynamic therapy  
In this regard, the usefulness of such nanostructures as carbon nanotubes and dendrimers has been confirmed.
- media in thermotherapy (hyperthermal)  
In oncology, hyperthermia is a therapy that uses the controlled rise of temperature to destroy cancer cells or inhibit their growth. The nanostructures such as gold nanoparticles (converting the near-infrared electromagnetic radiation into the heat energy) or superparamagnetic iron oxide nanoparticles (generating heat under the influence of the external magnetic field) have been used here. The therapy using the conjugate of gold nanoparticles and paclitaxel, followed by the IR irradiation is of particular interest because of the confirmed synergy effect (cells resistant to paclitaxel alone may have been killed by hyperthermia and vice versa).
- the radiosensitizer in the radiotherapy  
The cited works showed that gold nanoparticles increased the sensitivity of cancer cells to the X-ray. The therapy using the conjugate of gold nanoparticles and cisplatin in combination with radiotherapy on the glioblastoma multiforme is a promising solution.

In conclusion, the studies so far give hope for the development of new drugs and therapeutic methods with more selective and less toxic effects. However, further research on the fundamental biological processes in cancer and pharmacokinetics, as well as the metabolism and toxicity of the nanostructures in the biological systems seems to be necessary.

## ORCID iDs






- D. Laskowska:  <https://orcid.org/0000-0002-0047-8878>  
 E. Ziolkowska:  <https://orcid.org/0000-0001-7348-0189>  
 K. Mitura:  <https://orcid.org/0000-0002-2658-2542>

## References

- [1] Mazurkiewicz A.: Nanonauki i nanotechnologie. Stan i perspektywy rozwoju. Wydawnictwo Instytutu Technologii Eksploatacji - Państwowy Instytut Badawczy, Radom 2007
- [2] Sokół J.L.: Nanotechnologia w życiu człowieka. *Ekonomia i Zarządzanie* 4 (2012) 18-29.
- [3] Dębek P., Feliczak-Guzik A., Nowak I.: Nanostruktury - ogólne informacje. Zastosowanie nanoobjektów w medycynie i kosmetologii. *Postępy Hig Med Dosw* 71 (2017) 1055-1062.
- [4] Runowski M.: Nanotechnologia - nanomateriały, nanocząstki i wielofunkcyjne nanostruktury typu rdzeń/powłoka. *CHEMIK* 68 (2014) 766-775.
- [5] Yu K.M., Park J., Jon S.: Targeting Strategies for Multifunctional Nanoparticles in Cancer Imaging and Therapy. *Theranostics* 2 (2012) 3-44.
- [6] Wolska K.I., Markowska K., Wypij M., Golińska P., Dahm H.: Nanocząstki srebra, synteza i biologiczna aktywność. *KOSMOS Problemy Nauk Biologicznych* 66 (2017) 125-138.
- [7] Popowska M.: Antybiotykoodporność w środowisku naturalnym-przyczyny i konsekwencje. *KOSMOS Problemy Nauk Biologicznych* 66 (2017) 81-91.
- [8] Rzeszutek J., Matysiak M., Czajka M., Sawicki K., Rachubik P., Kruszewski M., Kapka-Skrzypczak L.: Zastosowanie nanocząstek i nanomateriałów w medycynie. *Hygeina Public Health* 49 (2017) 449-457.
- [9] Pulit J., Banach M., Kowalski Z.: Właściwości nanocząstek miedzi, platyny, srebra złota i palladu, *Czasopismo Techniczne. Chemia* 10 (2011) 197-209.
- [10] Dyla J.: Zastosowanie nanośników w medycynie. *CHEMIK* 67 (2013) 11-14.
- [11] Śliwińska-Hill U., Celmer J., Trynda-Lemiesz L.: Związki złota jako potencjalne leki przeciwnowotworowe nowej generacji. *NOWOTWORY Journal of Oncology* 63 (2013) 456-462.
- [12] Błaszczak-Świątkiewicz K., Olszewska P., Mikiciuk-Olasik E.: Zastosowanie nanocząsteczek w leczeniu i diagnostyce nowotworów. *NOWOTWORY Journal of Oncology* 63 (2013) 320-330.
- [13] Bituicki M., Sękowski S.: Nanocząsteczki złota w terapii przeciwnowotworowej. *KOSMOS Problemy Nauk Biologicznych* 65 (2016) 227-234.
- [14] Raj S., Khurana S., Choudhari R., Kesari K.K., Kamal M.A., Garg N., Ruokolainen J., Das B.C., Kumar D.: Specific targeting cancer cell with nanoparticles and drug delivery in cancer therapy. *Seminars in Cancer Biology* (2019), <https://doi.org/10.1016/j.semcancer.2019.11.002>
- [15] Cho K., Wang X., Nie S., Chen Z.G., Shin D.M.: Therapeutic Nanoparticles for Drug Delivery in Cancer. *Clin Cancer Res* 14 (2008) 1310-1316.
- [16] Rodallec A., Benzekary S., Lacarelle B., Ciccolini J.: Pharmacokinetics variability: Why nanoparticles are not just magic-bullets in oncology. *Critical Reviews in Oncology / Hematology* 129 (2018) 1-12.
- [17] Werengowska K.M., Wiśniwski M., Terzyk A.P., Gurtowska N., Drewa T.A., Olkowska J.: Chemiczne aspekty celowanej terapii przeciwnowotworowej II. Połączenia nośnik-lek, *Wiadomości Chemiczne* 66 (2012) 638-670.
- [18] Tiwari P.M., Vig K., Dennis V.A., Singh S.R.: Functionalized Gold Nanoparticles and Their Biomedical Applications. *Nanomaterials* 1 (2011) 31-63.
- [19] Mirza Z., Karim S.: Nanoparticles-based drug delivery and gene therapy for breast cancer: Recent advancements and future challenges. *Seminars in Cancer Biology* (2019), <https://doi.org/10.1016/j.semcancer.2019.10.020>
- [20] Mielcarek J., Kruszyńska M., Sokołowski P.: Zastosowanie nanorurek węglowych w medycynie. *Farm Pol* 65 (2009) 251-254.
- [21] Mielcarek J., Skupin P.: Biomedyczne zastosowania i toksyczność nanorurek węglowych. *Farm Pol* 65 (2009) 407-410.
- [22] Liu Z., Chen K., Davis C., Sherlock S., Cao Q., Chen X., Dai H.: Drug delivery with carbon nanotubes for *in vivo* cancer treatment. *Cancer Res* 68 (2008) 6652-6660.
- [23] Wiśniwski M., Rossochacka P., Werengowska-Ciećwierz K., Bielecja A., Terzyk A.P., Gauden P.A.: Medyczne aspekty nanostrukturalnych materiałów węglowych. *Inżynieria i Ochrona Środowiska* 16 (2013) 255-261.
- [24] Tripisciano C., Kraemer K., Taylor A., Borowiak-Palen E.: Single-wall carbon nanotubes based anticancer drug delivery system. *Chemical Physics Letters* 478 (2009) 200-205.
- [25] Tripisciano C., Costa S., Kalenczuk R.J., Borowiak-Palen E.: Cisplatin filled multiwalled carbon nanotubes - a novel molecular hybrid of anticancer drug container. *The European Physical Journal B* 75 (2010) 141-146.
- [26] Hampel S., Kunze D., Haase D., Kramer K., Rauschenbach M., Ritschel M., Leonhardt A., Thomas J., Oswald S., Hoffmann V., Buchner B.: Carbon nanotubes filled with a chemotherapeutic agent: a nanocarrier mediates inhibition of tumor cell growth. *Nanomedicine (London)* 3 (2008) 175-182.
- [27] Ali-Boucetta H., Al-Jamal K.T., McCarty D., Maurizio P., Bianco A., Kostarelos K.: Multiwalled carbon nanotube-doxorubicin supramolecular complexes for cancer therapeutics. *Chemical Communications* 8 (2008) 459-461.
- [28] Yan J., Xue F., Chen H., Wu X., Zhang H., Chen G., Lu J., Cai L., Xiang G., Deng Z., Zheng Y., Zheng X., Li G.: A multi-center study of using carbon nanoparticles to track lymph node metastasis in T1-2 colorectal cancer. *Surgical endoscopy* 28 (2014) 3315-3321.
- [29] Yang S.T., Luo J., Zhou Q., Wang H.: Pharmacokinetics, Metabolism and Toxicity of Carbon Nanotubes for Biomedical Purposes. *Theranostics* 2 (2012) 271-282.
- [30] Kubiak M.: Dendrymery- fascynujące nanocząsteczki w zastosowaniu w medycynie. *CHEMIK* 68 (2014) 141-150.
- [31] Sękowski S., Miłowska K., Gabryelak T.: Dendrymery w naukach biomedycznych i nanotechnologii. *Postępy Higieny i Medycyny Doświadczalnej* 62 (2008) 725-733.
- [32] Agostinis P., Berg K., Cengel K.A., Foster T.H., Girotti A.W., Gollnick S.O., Hahn S.M., Hamblin M.R., Juzeniene A., Kessel D., Korbelik M., Moan J., Mróz P., Nowis D., Piette J., Wilko B.C., Gołąb J.: Photodynamic therapy of cancer: an update. *CA Cancer J Clin.* 61 (2011) 250-281.
- [33] Khabashesku V.N., Margrave J.L., Barrera E.V.: Functionalized Carbon Nanotubes and Nanodiamonds for Engineering and Biomedical Applications. *Diamond and Related Materials* 14 (2005) 859-866.
- [34] Rzepka E., Pusküllüoglu M.: Znaczenie hipertermii w leczeniu onkologicznym. *Onkol. Prak. Klin.* 8 (2012) 178-188.
- [35] Kennedy L.C., Bickford L., Lewinski N.A., Coughlin A.J., Hu Y., Day E.S., West J.L., Drezek R.A.: A New Era for Cancer Treatment: Gold-Nanoparticle Mediated Thermal Therapies. *Small* 7 (2011) 169-183.
- [36] Peralta D.V., Heidari Z., Dash S., Tarr M.A.: Hybrid paclitaxel and gold nanorod-loaded human serum albumin nanoparticles for simultaneous chemotherapeutic and photothermal therapy on 4T1 breast cancer cells. *ACS Appl Mater Interfaces* 7 (2015) 7101-7111.
- [37] Jurczyk M.: Termoterapia z użyciem magnetycznych nanocząstek. *Curr. Gynecol. Oncol.* 8 (2010) 82-89.
- [38] Zhao Q., Wang L., Cheng R., Leidong M., Arnold R.D., Howerth E. W., Chen Z. G., Platt S.: Magnetic Nanoparticles-Based Hyperthermia for Head & Neck Cancer in Mouse Models. *Theranostics* 2 (2012) 113-121.
- [39] Rahman W.N., Bishara N., Ackerly T., He C.F., Jackson P., Wong C., Davidson R., Geso M.: Enhancement of radiation effects by gold nanoparticles for superficial radiation therapy. *Nanomed Nanotechnol Biol Med.* 5 (2009) 136-142.
- [40] Geng F., Song K., Xing J.Z., Yuan C., Yan S., Yang Q., Chen J., Kong B.: Thio-glucose bound gold nanoparticles enhance radio-cytotoxic targeting of ovarian cancer. *Nanotechnology* 22 (2011) 285101.
- [41] Roa W., Zhang X., Guo L., Shaw A., Hu X., Xiong Y., Glavita S., Patel S., Sun X., Chen J., Moore R., Xing J.Z.: Gold nanoparticle sensitize radiotherapy of prostate cancer cells by regulation of the cell cycle. *Nanotechnology* 20 (2009) 375101.
- [42] Setua S., Ouberaï M., Piccirillo S.G., Watts C., Welland M.: Cisplatin-tethered gold nanospheres for multimodal chemoradiotherapy of glioblastoma. *Nanoscale* 6 (2014) 10865-10873.



# SYNTHETIC EXTRACELLULAR MATRIX AS A SUBSTRATE FOR REGENERATIVE MEDICINE

EWA STODOLAK-ZYCH<sup>1\*</sup> , ELŻBIETA MENASZEK<sup>2</sup> ,  
ALEKSANDRA TWARDY<sup>1</sup>, ANNA ŚCISŁOWSKA-  
CZARNECKA<sup>3</sup> , MACIEJ BOGUŃ<sup>4</sup> ,  
BEATA KOLESIŃSKA<sup>5</sup> 

<sup>1</sup> DEPARTMENT OF BIOMATERIALS AND COMPOSITES,  
FACULTY OF MATERIALS SCIENCE AND CERAMICS,  
AGH UNIVERSITY OF SCIENCE AND TECHNOLOGY,  
AL. MICKIEWICZA 30, 30-059 KRAKÓW, POLAND

<sup>2</sup> DEPARTMENT OF CYTOBIOLOGY, COLLEGIUM MEDICUM,  
JAGIELLONIAN UNIVERSITY,  
UL. MEDYCZNA 9, 30-688 KRAKÓW, POLAND

<sup>3</sup> DEPARTMENT OF PHYSIOTHERAPY,  
ACADEMY OF PHYSICAL EDUCATION,  
AL. JANA PAWŁA II 28, 31-571 KRAKÓW, POLAND

<sup>4</sup> THE ŁUKASIEWICZ RESEARCH NETWORK -  
TEXTILE RESEARCH INSTITUTE,  
UL. BRZEZIŃSKA 5/15, 92-103 ŁÓDŹ, POLAND

<sup>5</sup> INSTITUTE OF ORGANIC CHEMISTRY,  
LODZ UNIVERSITY OF TECHNOLOGY,  
UL. S. ŻEROMSKIEGO 116, 90-924 ŁÓDŹ, POLAND

\*E-MAIL: STODOLAK@AGH.EDU.PL

## Abstract

The work presents materials characteristics of fibrous polysaccharide substrates (calcium alginate, CA) modified with short peptides. Three types of synthesized peptides (hexapeptides) were composed of: cysteine (C) and tryptophan (W) named - (WWC)<sub>2</sub> or cysteine (C) and tyrosine (Y) named (YYC)<sub>2</sub> or phenylalanine (F) named 6F. The peptides size distribution (DLS method) showed that they agglomerated in an alcohol medium. These results were used to select a modification method of the fibrous substrates i.e. the peptides were deposited on the fibrous alginate substrate by the electrospraying technique. Using this method three kinds of polysaccharide-peptides systems were obtained i.e.: CA/(WWC)<sub>2</sub>, CA/(YYC)<sub>2</sub>, CA/6F. As a reference material, the pure calcium alginate fibrous substrate was used.

The results of modification with short peptides were evaluated via scanning electron microscopy (SEM): small aggregates were observed (40-100 nm) on the surface of fibers, and the fibers size remained the same after modification (11-12 μm). The size of aggregates depended on the kind of short peptide; the smaller (40 nm) aggregates were observed when the peptide had only aromatic chain (6F), the bigger (<100 nm) ones were observed when the peptide had heterocyclic rings in the chain (WWC and YYC). All materials were contacted with osteoblast-like cells (MG-63) to test biocompatibility (cells viability after 3 and 7 days) and the results proved showed higher viability in the polysaccharide-peptide system which increased with the time of observation. The durability of polysaccharide-peptide systems was tested using the enzymatic assay: collagenase confirmed the stability of materials. The progress of degradation rate was observed using infrared spectroscopy (FTIR-ATR) - the ratio on bands with C-O and C-OH increased after degradation under in vitro conditions.

Results of the investigations on the fibrous substrates have confirmed that the system is a good model of an extracellular matrix (ECM) due to its chemical composition and microstructure which both have biomimetic characteristics. Thus, it may be used as a filling of bone defects supporting the regeneration of the damaged tissue. Additionally, it may also serve as the model research system of ECM.

**Keywords:** synthetic extracellular matrix, biomimetic, peptide, polysaccharides, laboratory model

[Engineering of Biomaterials 152 (2019) 10-15]

## Introduction

The extracellular matrix is a natural microenvironment for cells of all tissues constituting a living organism [1]. The main task of the matrix is not only to provide the cells with scaffolds but also to ensure such a location that enables the cells to pick transmitted signals. The proper communication via biochemical or biomechanical signals guarantees the maintenance of homeostasis as well as the correct course of morphogenesis or cell differentiation [2-3]. From the structural point of view, the fibrous matrix is composed of proteins and polysaccharides. Protein fibres, i.e. collagen and elastin, are enriched with non-fibrous forms, such as glycosaminoglycans (GAG), proteoglycans (PG) or free matrix proteins [4]. This specific fibrous composite consisting of biopolymers (proteins and polysaccharides) is a model that scientists attempt to reproduce in the laboratory conditions. Yet, the concept of using the natural ECM framework obtained via tissue decellularization poses many problems. The difficulties include the antigens removal, the risk of rejecting the scaffold after implantation and the destruction of fibers during the chemical treatment of ECM. Another issue is the lack of process repeatability. All the mentioned problems force scientists to research alternative solutions [1]. A new strategy is designing of a scaffold that will act as an extracellular framework and imitate the scaffolding structure and microstructure (biomimetic approach) [5-6]. A good example of biomimetic ECM scaffolds are polysaccharide fibers the microstructure modified with short peptides.

Fibrous scaffolds are attractive substrates stimulating cells to faster adhesion and proliferation. The interaction between cells and materials will be even more effective when the cells encounter peptides suitable for creating a chemical complex between the cell's plasma and the biomaterial's surface (FIG. 1).

The purpose of the work was to develop and characterize the fibrous substrate (matrix) produced from calcium alginate modified with short peptides. The deposition of peptides on the fibers surface was conducted by the electrospraying technique. The peptides used in the experiment were hexapeptides basing on tyrosine and cysteine (WWC)<sub>2</sub>, tryptophan and cysteine (YYC)<sub>2</sub> or phenylalanine (6F). The polysaccharide-peptides systems were subjected to both microstructural (via optical microscope, scanning electron microscope) and structural examinations (FTIR-ATR). Then the durability of the systems was assessed in the external environment of water and enzymes (collagenase). The tests revealed that all CA/peptide systems are characterized by microstructure stability (SEM), the high degree of soaking and durability during degradation processes (FTIR-ATR). Thus, they are a good research model to conduct experiments involving cells from continuous lines (MG-63).

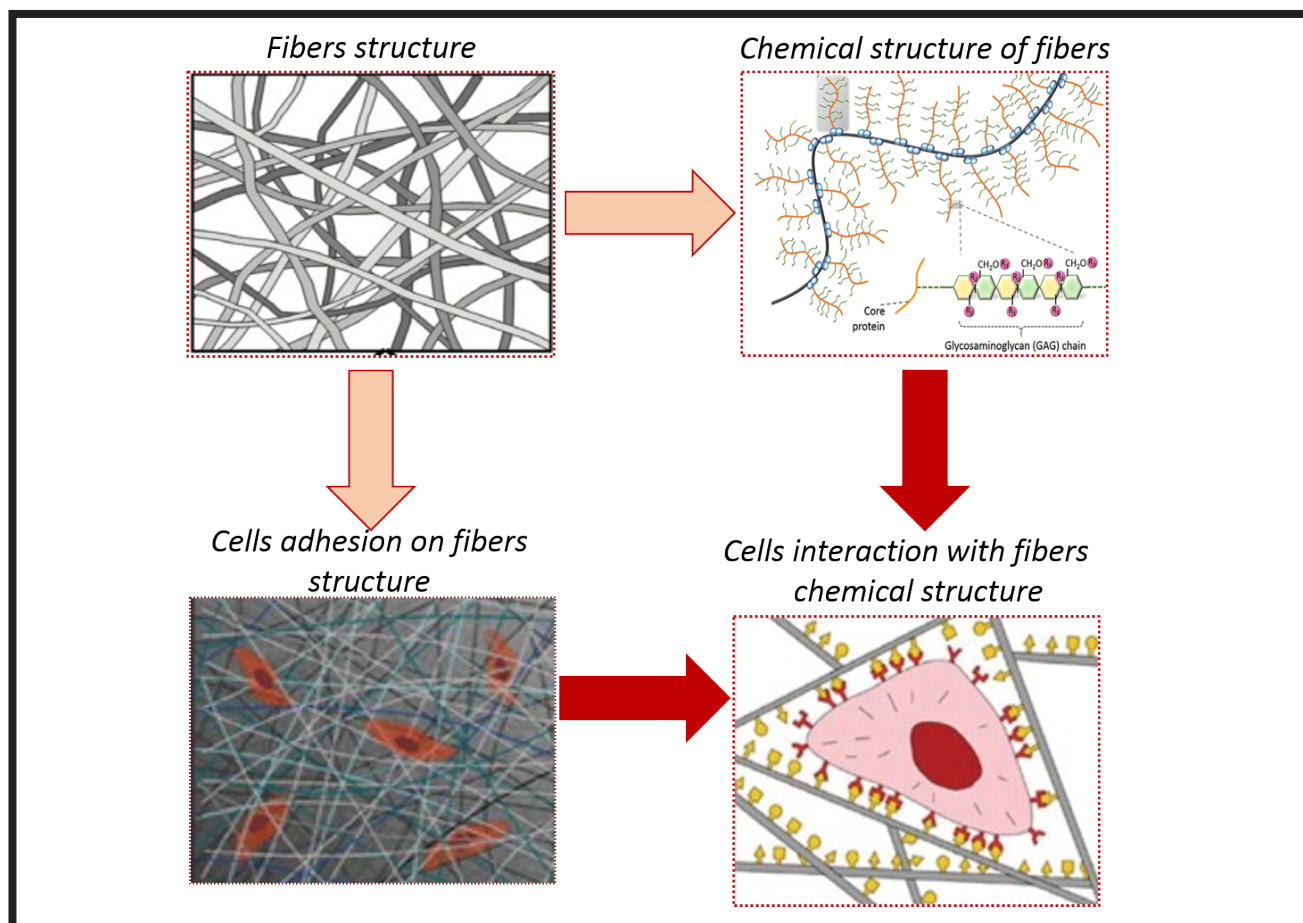


FIG. 1. The strategy of biomimetic, fibrous scaffolds with protein stimulated cells-materials interaction.

## Materials and Methods

The polysaccharide fibrous substrate made of calcium alginate was obtained by the method of extraction solution at the Faculty of Technology and Textile of the Lodz University of Technology. According to the methodology of this process, sodium alginate (Protanal 80/20, BioPolymers) was dissolved and homogenized to obtain a spinning solution. Next, the solution was passed through the spinneret directly into the precipitation bath (3% solutions of  $\text{CaCl}_2/\text{NaCl}$ ). Further, the calcium alginate (CA) fibers were washed with ethyl alcohol solutions of various concentrations (50, 70 and 90%) in order to remove residues of the precipitation bath. The short peptides were synthesized at the Institute of Organic Chemistry of the Lodz University of Technology. The first hexapeptide consisted of tryptophan (W) and cysteine (C), the second series of peptides included tyrosine (Y) and cysteine (C) and the third peptides contained phenylalanine (F). Some important data on the short peptides were presented in TABLE 1.

Due to solubility of all the peptides in the 70% solution of ethyl alcohol, the 0.5% w/wt. peptides solutions were prepared. In such conditions, the peptides size distribution was measured using the DLS method (Litesize 500 DLS, Anton-Paar).

The wettability of all the tested materials was characterized (DSA 25, Kruss). Ethyl alcohol (EtOH, Avantor SA) was used in this method as a liquid. The polysaccharide fibrous substrate was characterized by a swelling test, during which the alginate fibers were immersed in water at 37°C for 24 h. The mass changes and fibers size (SEM, Nova NanoSEM) were observed after the swelling. Finally, using the electrospinning method (the apparatus settings: voltage 15 kV, application time 10 min, chamber temperature 37°C) – the peptides solutions with alcohol (1% w/wt.) were applied. In this manner, a series of the substrates based on calcium alginate fibers modified with three different hexapeptides was developed for the tests. The calcium alginate fibers were selected as the polysaccharide reference material. The microstructural characteristics of the initial and the modified fibers was performed using SEM microscopy (Nova NanoSEM, FEI). The polysaccharide-peptides systems were also tested for enzymatic degradation process in order to check their *in vitro* stability. The concentration of ions in the immersion medium (Ringer solution/37°C/3 months) and the concentration of collagenase (in the Tracine buffer) were monitored during the incubation [7]. The progress of the enzymatic degradation process was assessed by the infrared spectroscopy (FTIR-ATR) after the degradation process.

TABLE 1. Characteristics of short peptides: compositions, size, and wettability.

peptide	name	size, DLS [nm]	wettability, theta [°]
WWCWWC	(WWC) <sub>2</sub>	112.8	39.4 ± 5.6
YYCYCY	(YYC) <sub>2</sub>	391.3	38.7 ± 3.9
FFFFFF	6F	40.5	69.4 ± 5.4



## Results and Discussion

The short peptides were well pre-wetted by ethyl alcohol (wetting angle about 40° for mixed hexapeptides, for a peptide composed of the same amino acids the wetting angle was about 70°). The peptides slowly and partially dissolve in an alcoholic medium and the higher solubility was obtained when they were heated to about 30°C. This was a short-term effect because the decrease in temperature below 30°C again caused the strong peptides agglomeration (as seen in the results of the particle size distribution, TABLE 1). The short peptides used in the experiment have aromatic rings in their structure (tyrosine - an indole ring, tyrosine - a phenolic ring) which facilitate the process of rolling back. It is known that peptide chains enriched with tyrosine or tryptophan are twisted to  $\beta$ -harmonic [8]. Such a phenomenon is not observed for peptides rich in phenylalanine (the smallest agglomerates in hexapeptide 6F are about 40 nm). The tested fibrous materials are supposed to serve as scaffolds implanted into the human body.

Therefore, they should be characterized by a high level of water absorption. The obtained results indicated that, regardless of the kind of the applied peptide, all substrates displayed the water absorption higher than 300% (TABLE 2). This was confirmed by the hydrogel character of calcium alginate [9].

The neat CA fibers had a diameter of 11-12  $\mu\text{m}$  and their surface was quite regular and smooth. The selected method of the substrates fabrication resulted in the multi-directional fiber-distribution with pores located among them. The application of the peptides did not cause significant alterations to the fiber morphology and diameter (FIG. 2). In the case of the fibers modified with hexapeptide (6F) it was very difficult to find aggregates (particles size of the peptide was about 40 nm). However, new forms appeared on the surface - the aggregates of the respective peptides (FIG. 2: CA/(WWC)<sub>2</sub>, CA/(YYC)<sub>2</sub>). The peptides with an indole ring (e.g. tryptophan) were more prone to form irregular stack forms or  $\beta$ -sheet [10-11]. On the other hand, the tyrosine-based peptides (a phenolic ring) did not show such tendencies [12], so they formed more irregular shapes.

**TABLE 2. Composition and physical properties of compositions based on nonwoven fibers (calcium alginate, CA) modified with the short peptides.**

Samples name	Swelling [%]	Fiber diameter, before degradation [ $\mu\text{m}$ ]	Fiber diameter after degradation [ $\mu\text{m}$ ]
CA	320	10.92 $\pm$ 1.28	10.54 $\pm$ 1.61
CA/(WWC) <sub>2</sub>	210	11.99 $\pm$ 1.25	11.47 $\pm$ 1.76
CA/(YYC) <sub>2</sub>	280	11.59 $\pm$ 1.39	11.28 $\pm$ 2.04
CA/6F	300	11.97 $\pm$ 2.37	11.56 $\pm$ 2.84

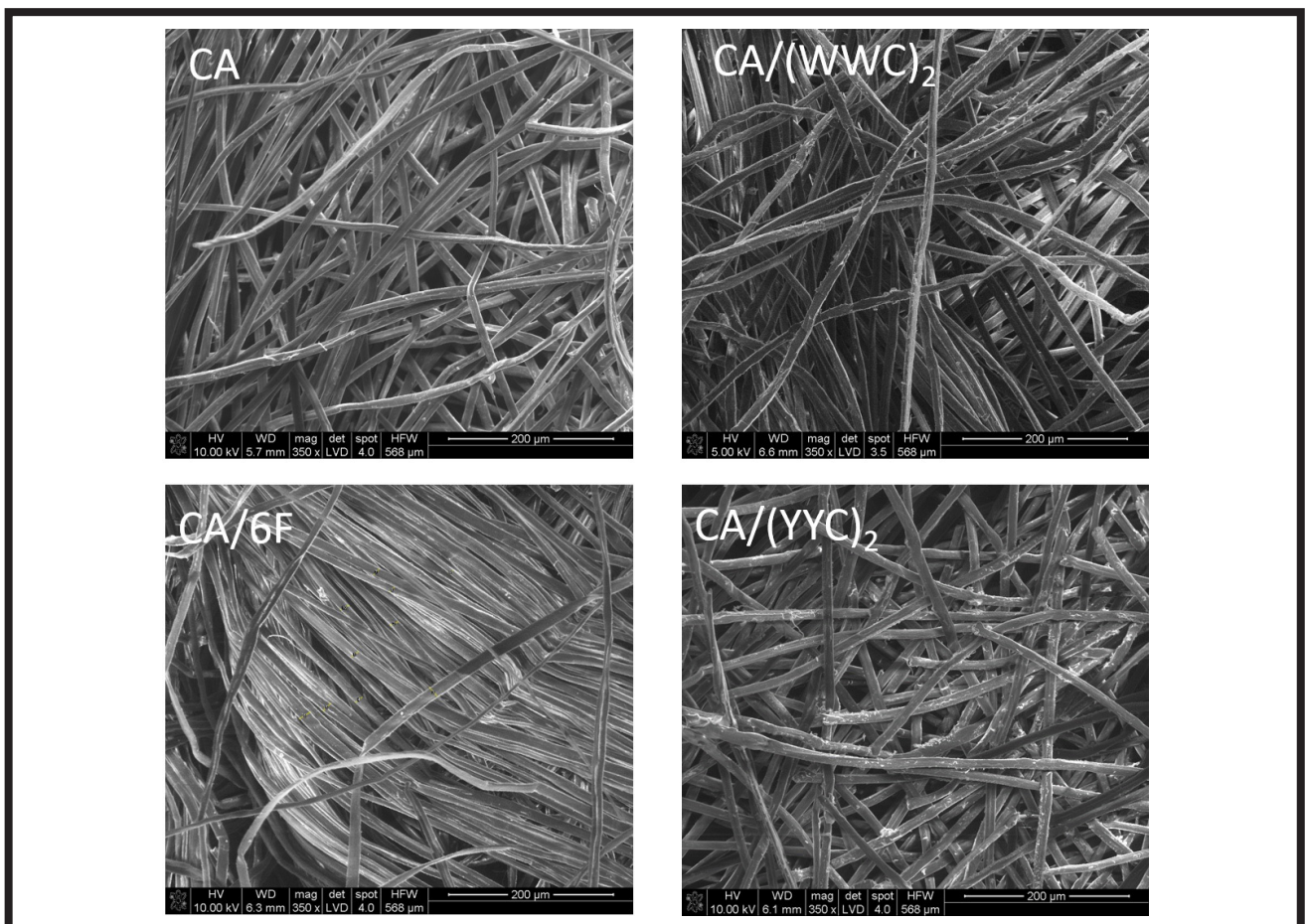


**FIG. 2. The microstructure of the fibrous scaffold modified with the short peptides.**



The peptides presence on the fibers was confirmed not only by the change in morphology but also by the subtle changes in the CA spectrum (FIG. 3a). The bands in the range 1100-1350  $\text{cm}^{-1}$  proved the presence of the ring in the peptide (more visible in the first derivative). The bands ranging 3400-3600  $\text{cm}^{-1}$  were evidence of the peptide bonds (amide 1 $^\circ$  and 2 $^\circ$ ). Their intensity was relatively smaller than the intensity of the bands originating from the substrate, which resulted from a small amount of the applied peptide. A change in the matrix morphology resulted from the hydrolytic degradation conducted for 4 months in enzymes (collagenase in Tracine buffer). Namely, the fibers became rough and the aggregates of proteins were more difficult to recognize. The fibers diameters did not change (TABLE 2) but their surface was less homogeneous. Probably the polysaccharides-peptide interaction had only the electrostatic or hydrogen bond character, hence the change in the external environment caused the relaxation of these interactions.

The peptides ( $\text{WWC}$ )<sub>2</sub> were able to penetrate inside the fiber, as it was evidenced by the changes in the FTIR-ATR spectra taken for the degraded materials (FIG. 3b). In the fiber itself, the bands at 1200  $\text{cm}^{-1}$  were observed for the tyrosine systems, whereas sulphur ions (derived from cysteine) were found in the incubation solution.

The ion concentration was higher if the tryptophan-based systems (YYCYC) or the tyrosine base system (WWCWWC) were used for the modification. The previous study showed that the hydrolytic degradation conducted in the Ringer solution (RS) resulted in dissolving the polysaccharide substrate. This phenomenon confirmed the assumption that calcium alginate fibers in the presence of cations (derived from PBS) got substituted, forming the systems of sodium alginate with salt soluble in water [9]. The examined peptides did not dissolve in the Ringer solution; therefore, they did not undergo the enzymatic degradation [13].

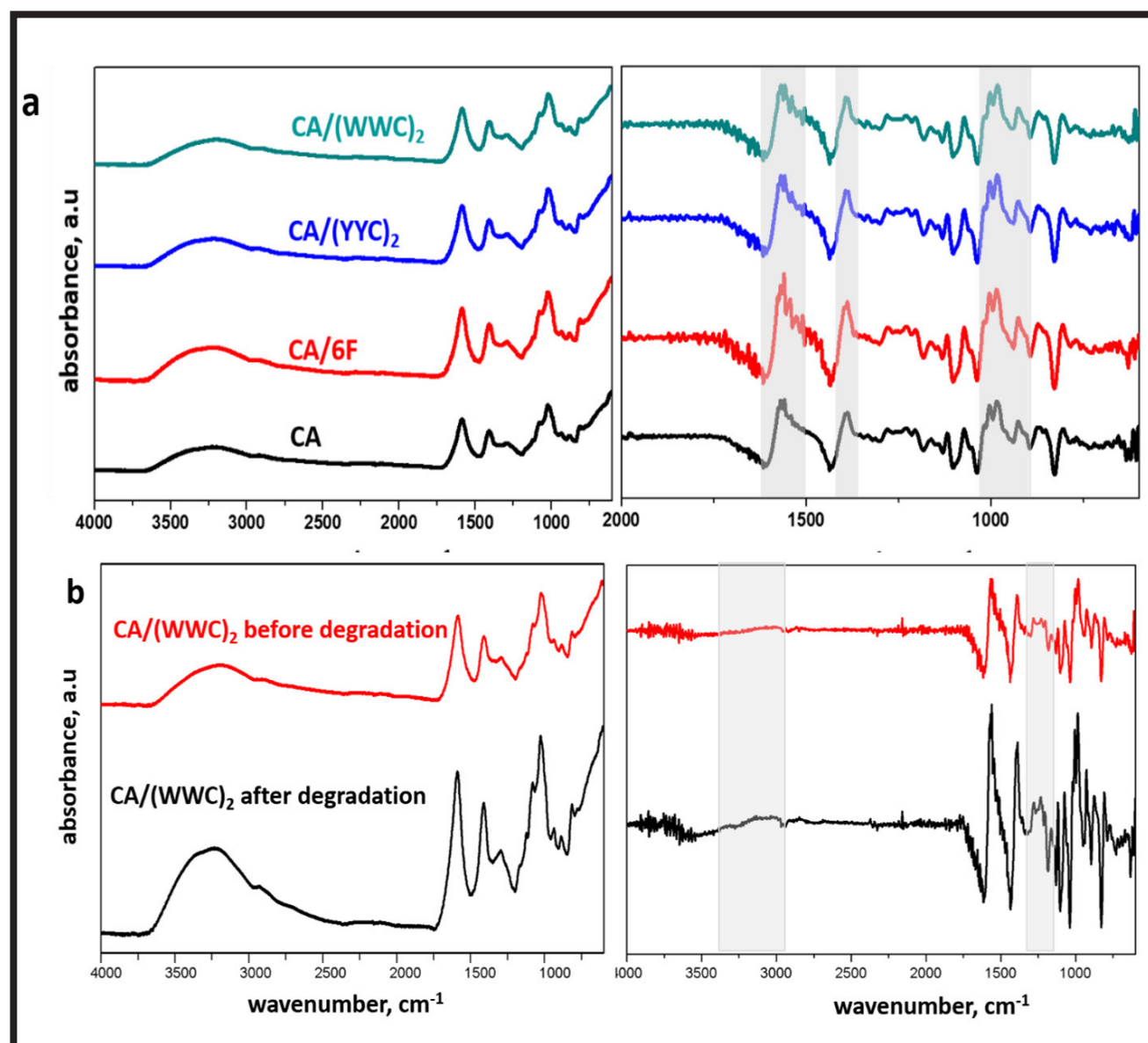


FIG. 3. FTIR-ATR spectra of polysaccharides-peptides system: (a) after modification with peptides WWC, YYC 6F (conventional spectrum, the first derivatives of spectra), (b) after degradation CA/(WWC)<sub>2</sub> (conventional spectrum, the first derivative of the spectrum).

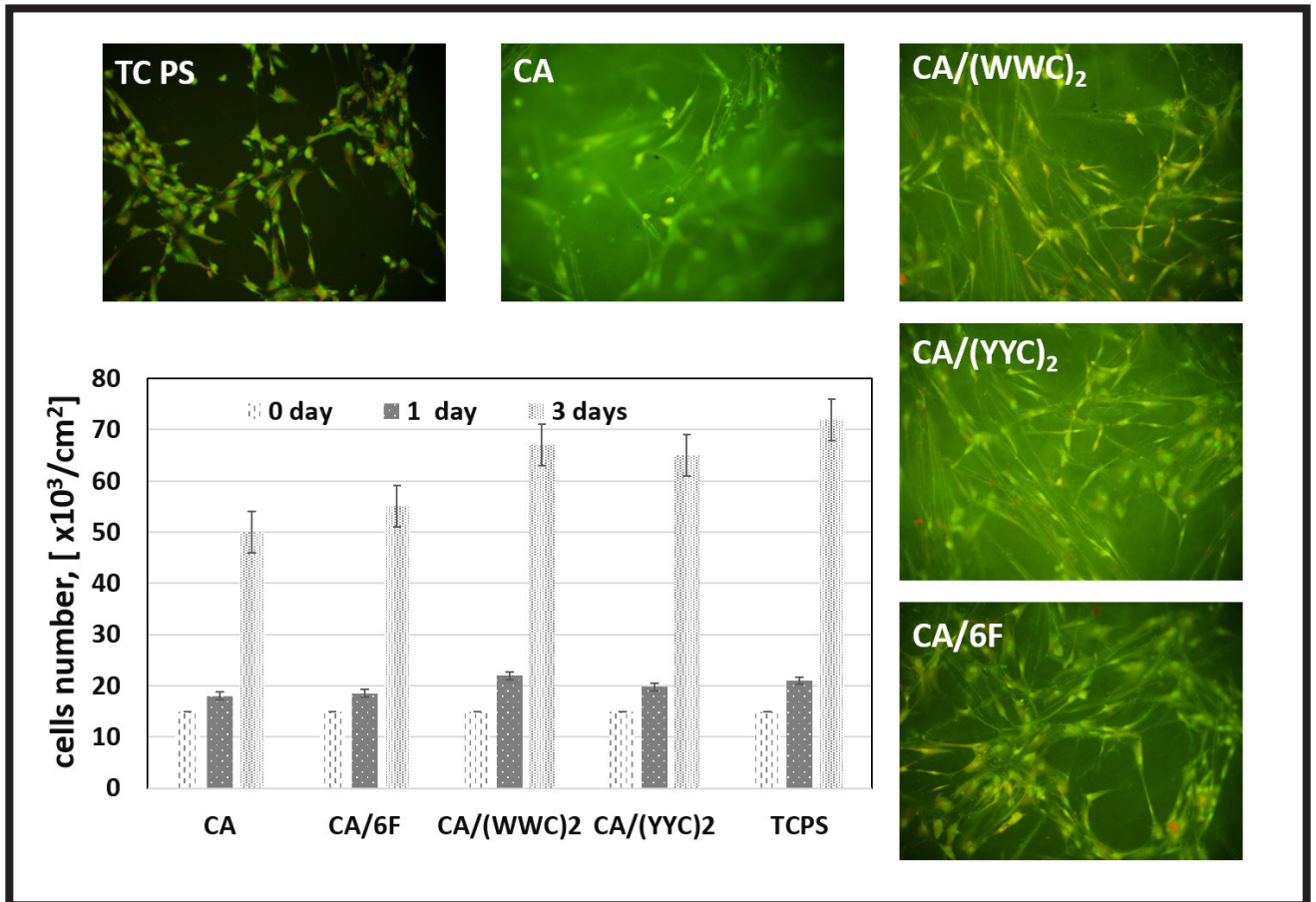


FIG. 4. Viability of MG-63 cells after 1-day and 3-days incubation and their morphology on the fibrous scaffolds observed in 3 days.

Due to their high wettability, the peptide-polysaccharides systems were not easy to conduct experiments on. The gel base made it difficult to observe the morphology of MG-63 cells. However, the quantitative determination of the cells confirmed the good biocompatibility of the tested materials after the 1- and 3-day incubation periods (FIG. 4). The most advantageous results were obtained for the fibers modified with tyrosine-based peptides. Tyrosine is an amino acid that is sparingly soluble in water, yet it is necessary for proper metabolism [14]. Introducing the additional amount of tyrosine into the system did not affect its environmental stability or cell functions (admissible amount of tyrosine in CCM is 0.029-0.197 g/L) [15]. In turn, the presence of tryptophan may influence the physicochemical properties of the substrate (decrease its wettability), supporting the metabolic processes associated with the cell spreading [16].

## Conclusions

The tested protein-sugar systems derived from calcium alginate and synthetic short peptides constitute a promising group of *in vitro* stable substrates.

Taking into account the morphology and structure, the calcium alginate modified with the peptides (WWC)<sub>2</sub> and (YYC)<sub>2</sub> mimics the polysaccharide-peptide systems that build the extracellular matrix.

Due to their durability, the examined materials can be used as models for biological tests aimed at the microstructure improvement (making it more biomimetic).

They may also be used in further research to assess the possibilities of supporting regenerative processes.

## Acknowledgements

This work was supported by the National Science Center, Poland, under grant no. UMO-2015/19/B/ST8/02594.

### ORCID iDs

- E. Stodolak-Zych: <https://orcid.org/0000-0002-8935-4811>  
 E. Menaszek: <https://orcid.org/0000-0002-0602-3583>  
 A. Ścisłowska-Czarnecka: <https://orcid.org/0000-0001-8398-8912>  
 M. Boguń: <https://orcid.org/0000-0001-7436-4219>  
 B. Kolesińska: <https://orcid.org/0000-0002-4581-947X>

## References

- [1] Hinderer S., Layland S.L., Schenke-Layland K.: ECM and ECM-like materials – biomaterials for applications in regenerative medicine and cancer therapy. *Adv. Drug Delivery Rev.* 97 (2016) 260-269.
- [2] Bačáková L., Novotná K., Pařízek M.: Polysaccharides as cell carriers for tissue engineering: the use of cellulose in vascular wall reconstruction. *Physiol. Res.* 63 (2014) 29-47.
- [3] Jabłońska-Trypuć A., Matejczyk M., Rosochacki S.: Matrix metalloproteinases (MMPs), the main extracellular matrix (ECM) enzymes in collagen degradation, as a target for anticancer drugs. *J. Enzyme Inhib. Med. Chem.* 31(S1) (2016) 177-183.
- [4] Yue B.: Biology of the Extracellular Matrix: An Overview. *J. Glaucoma* 23 (2014) 20-23.
- [5] Kuttappan S., Mathew D., Nair M.B.: Biomimetic composite scaffolds containing bioceramics and collagen/gelatin for bone tissue engineering – A mini review. *Int. J. Biol. Macromol.* 93 (2016) 1390-1401.
- [6] Wu J., Xie L., Zhi W., Lin Y., Chen Q.: Biomimetic nanofibrous scaffolds for neural tissue engineering and drug development. *Drug Discovery Today* 22(9) (2017) 1375-1384.
- [7] Protocol: Enzymatic Assay of Collagenase (EC 3.4.24.3) using FALGPA (N-(3-[2-Furyl]acryloyl)-Leu-Gly-Pro-Ala) as the Substrate. Sigma-Aldrich, 2017.
- [8] Chaberska A., Fraczyk J., Wasko J., Rosiak P., Kaminski Z.J., Sołecka A., Stodolak-Zych E., Strzempek W., Menaszek E., Dudek M., Niemiec W., Kolesinska B.: Study on the materials formed by self-assembling hydrophobic aromatic peptides dedicated to be used for regenerative medicine. *Chem Biodivers.* 16(3) (2019) e1800543.
- [9] Stodolak E., Paluszkiwicz C., Boguń M., Błażewicz M.: Nanocomposite fibres for medical applications. *J. Mol. Struct.* 208 (2009) 924-926.
- [10] Anjana R., Vaishnavi M.K., Sherlin D., Kumar S.P., Naveen K., Kanth P.S., Sekar K.: Aromatic-aromatic interactions in structures of proteins and protein-DNA complexes: a study based on orientation and distance. *Bioinformation* 8(24) (2012) 1220-1224.
- [11] Kannan N., Vishveshwara S.: Aromatic clusters: a determinant of thermal stability of thermophilic proteins. *Protein Eng.* 13 (2000) 753-761.
- [12] Fraczyk J., Lipiński W., Chaberska A., Wasko J., Roźniakowski K., Kaminski Z.J., Boguń M., Draczynski Z., Menaszek E., Stodolak-Zych E., Kaminska M., Kolesinska B.: Search for fibrous aggregates potentially useful in regenerative medicine formed under physiological conditions by self-assembling short peptides containing two identical aromatic amino acid residues. *Molecules* 23 (2018) 568, 1-19.
- [13] Pace C.N., Treviño S., Prabhakaran E., Scholtz J.M.: Protein structure, stability and solubility in water and other solvents. *Philosophical Transactions of the Royal Society B. Biological Science.* 359 (2004) 1225-1235.
- [14] Salazar A., Keusgen M., von Hagen J.: Amino acids in the cultivation of mammalian cells. *Journal of Amino Acids* 48(5) (2016) 1161-1171.
- [15] Landauer K.: Designing media for animal cell culture: CHO cells, the industrial standard. *Methods Mol. Biol.* 1104 (2014) 89-103.
- [16] Carrillo-Cocom L.M., Genel-Rey T., Araiz-Hernandez D., Lopez-Pacheco F., Lopez-Meza J., Rocha-Pizana M.R., Ramirez-Medrano A., Alvarez M.M.: Amino acid consumption in naive and recombinant CHO cell cultures: producers of a monoclonal antibody. *Cytotechnology.* 67(5) (2014) 809-820.



# DEVELOPMENT OF A NEW PRODUCTION METHOD OF FOAM-LIKE WOUND DRESSINGS FOR SKIN REGENERATION

VLADYSLAV VIVCHARENKO , PAULINA KAZIMIERCZAK ,  
MICHAŁ WÓJCIK , AGATA PRZEKORA\* 

DEPARTMENT OF BIOCHEMISTRY AND BIOTECHNOLOGY,  
MEDICAL UNIVERSITY OF LUBLIN,  
20-400 LUBLIN, POLAND

\*E-MAIL: AGATA.PRZEKORA@UMLUB.PL

## Abstract

*Chitosan is widely used to prepare films, hydrogels, cryogels, sponges, fibers and other various biomaterials used in the tissue engineering field. It is one of the best processable polysaccharides used in biomedicine. However, its stability is generally lower as compared with others, due to its pH sensitivity and hydrophilic character. Using chitosan in combination with agarose may not only improve chemical and mechanical properties of the resultant material (by the formation of a biocomposite), but also lead to the formation of a gel imitating physical attributes of the extracellular matrix. Moreover, the combination of these two polysaccharides has a promising ability to improve the stability of chitosan and to increase fibroblasts' affinity to agarose. Characteristic advantageous features of these natural polymers raise a wide interest in tissue engineering. The aim of this study was to develop and optimize a new method to produce a highly biocompatible foam-like chitosan/agarose wound dressing for skin healing applications. The production process optimization helped to obtain the absorbent foam-like biomaterial which is non-toxic to skin fibroblasts and does not conduce their adhesion. Employing sodium bicarbonate as the main agent in the foaming reaction not only led to obtaining the foam-like structure but also neutralized the acidic pH, making the material non-toxic and non-irritating to the skin. In conclusion, the new foam-like biomaterial has great potential for biomedical applications as the wound dressing accelerating the healing process of the damaged tissues.*

**Keywords:** chitosan, agarose, biomaterials, fibroblasts, cytotoxicity

[*Engineering of Biomaterials 152 (2019) 16-20*]

## Introduction

Skin is the biggest organ in the human body that possesses numerous functions essential for human survival. The primary one is to keep a barrier between the external and internal environment [1]. The wounded epidermis is known to stimulate self-regeneration, but the healing process depends on the type of injury. If the regeneration is not adequate, it may lead to the formation of a chronic wound. Any deep wound resulting in full-thickness skin loss needs grafting for its cure [2]. Frequently, patients with a high percentage of injuries or burns cannot become a donor for self-skin transplantation. Therefore, surgery procedures are often limited by the low accessibility of healthy tissue.

Another strategy applied in skin regeneration is the allogeneic skin graft. Nevertheless, non-self-tissues used for allografts may cause immune rejection and infections related to the poor compatibility of tissue. Thus, in the case of extensive injuries or burn wounds, tissue-engineered skin grafts are the best way to overcome the above-mentioned problems [3,4]. The tissue engineering aims to fix, restore, improve or maintain tissue functions that have been lost due to various pathological conditions. The main strategies used can be classified into three primary groups: (1) implantation of the patient cells, (2) implantation of the different scaffolds seeded with patient cells, and (3) supplying tissue-inducing substances [5]. The development of appropriate scaffold design and an effective fabrication method is an important issue in regenerative medicine research and tissue engineering [6]. Among all engineered organs, the skin was the first tissue-engineered product used in patient treatment [7]. Over the last several decades, various natural and synthetic biomaterials for skin regeneration have been developed. A vast majority of them possess basic features of a proper wound dressing i.e. providing an external barrier against microorganisms, controlling the pain, removing exudates and also promoting the skin healing process [8].

Tissue-engineered biomaterials for skin regeneration that are currently available on the world market differ in a few main attributes: the type of biomaterial regarding its function (skin substitute/graft or external dressing), the duration of skin wound coverage (permanent or temporary), and cellular or acellular applications [9]. Interactive (or bioactive) dressings, like hydrogels (e.g. made of alginate, collagen), hydrocolloids, foams, or transparent films (e.g. made of polyurethane) are semi-occlusive or occlusive dressings that are essential for maintaining optimum moisture. They are recommended because of their advantageous influence on the local cellular response [10]. All the mentioned biomaterials may perform various important functions during the skin regeneration process, such as pain alleviation, protection of periwound skin, removal of nonviable tissues and dead spaces [11]. In general, wound dressings made of natural products can improve the wound healing process thanks to their demulcent, emollient, astringent, and antioxidant properties [12]. For instance, fibrinogen, elastin, chitosan, and collagen are natural biocompatible polymers similar to natural molecules present in the human organism [13]. Due to their efficient bioactive properties, natural polymers better interact with the cells facilitating the healing process. Natural polymers which are used in skin regenerative medicine can be divided into three large groups: (1) polysaccharides (e.g. alginate, dextran, chitin, chitosan, cellulose, amylose, glycosaminoglycans), (2) polynucleotides (DNA, RNA), and (3) proteins (e.g. collagen, elastin, gelatine, silk, fibrinogen) [6]. Synthetic polymers used in wound dressing production represent the largest group of biodegradable polymers. They are widely used in tissue engineering as it is possible to adapt their capabilities to the specific applications. Moreover, such biomaterials exhibit a long shelf time and can be produced in large uniform quantities [14]. Biological properties of bioactive dressings can be also improved by impregnation with antimicrobial or debriding agents, e.g. polyhexamethylene biguanide, cadexomer iodine, crystal violet, silver sulfadiazine, etc. [15]. The presence of natural or synthetic polymers and growth factors or other bioactive agents in the modern wound dressings composition makes it possible to predict the changes in the wound environment and to enhance the healing process [16].

The porosity of the potential wound dressings is a very important feature. It not only provides high material absorption but it is also essential for the cell proliferation, nutrition and tissue vascularization of the skin substitutes seeded with patient cells [17]. The aim of this study was to develop a new production method of the foam-like chitosan/agarose-based wound dressing that can be potentially used in skin tissue regeneration. To obtain a foam-like structure, the freeze-drying method was combined with a gas foaming agent. The reaction of sodium bicarbonate with acetic acid generates carbon dioxide which promotes the formation of a highly porous structure:  $\text{CH}_3\text{COOH} + \text{NaHCO}_3 \rightarrow \text{CH}_3\text{COONa} + \text{H}_2\text{O} + \text{CO}_2\uparrow$ . To optimize the production process various concentrations of chitosan, sodium bicarbonate and acetic acid were investigated. The final biomaterials were obtained by lyophilization of the frozen samples. The described method, using sodium bicarbonate as the main agent in the foaming reaction, not only allowed obtaining a foam-like structure but also neutralized the acidic pH, making the material non-toxic and non-irritating to the skin. The obtained dressings were subjected to cytotoxicity tests with human fibroblasts using MTT assay and live-dead staining.

## Materials and Methods

### Materials

The chitosan powder (Mw 150kDa) of 75-85% deacetylation was purchased from Sigma-Aldrich Chemicals. The agarose powder with the 36°C melting point and  $\leq 10\%$  moisture content, sodium bicarbonate powder (MW 84.01 g/mol), phosphate-buffered saline, Eagle's Minimum Essential Medium (EMEM), penicillin, streptomycin, trypsin-EDTA,

sodium dodecyl sulphate, Thiazolyl Blue Tetrazolium Bromide (MTT), Live/Dead Cell Double Staining Kit were supplied by Sigma-Aldrich Chemicals. The foetal bovine serum was obtained from Pan-Biotech, whereas the normal human skin fibroblast cell line (BJ) was obtained from American Type Culture Collections (ATCC).

### Preparation of the biomaterials

To optimize the production process of wound dressings, chitosan, solvent (acetic acid) and gas-foaming agent (sodium bicarbonate) were applied at different concentrations. To prepare the foam-like materials, a predetermined amount of chitosan powder (based on the required concentration, see TABLE 1) was added to the acetic acid solution applied at a concentration of 0.5% (v/v) or 1% (v/v) respectively. A beaker with the dissolved chitosan was placed on a hot plate magnetic stirrer and the 2% (w/v) agarose was slowly added to the chitosan solution. The stirrer parameters were matched to the final dissolution of agarose (15 min, 300 rpm, 95°C). Then, the 1% (w/v) or 2% (w/v) sodium bicarbonate was added to the polysaccharide blend and mixed to obtain a foam-forming reaction. Having obtained a homogeneous mass, it was spread on the polystyrene surface. Finally, the produced samples were cooled down at 6°C before freezing at 80°C overnight. All the samples were lyophilized for 20 h in order to receive the foam-like biomaterials. A schematic figure of the preparation of chitosan/agarose-based biomaterials can be seen in FIG. 1. The fabricated B4 biomaterial revealing the most homogeneous structure was visualized using the stereoscopic microscope (Olympus SZ61TR).

**TABLE 1. Sample design and various components concentrations used during the production process of chitosan/agarose biomaterials.**

Sample designation	Concentrations (%)				Observation
	Chitosan (w/v)	Agarose (w/v)	Acetic acid (v/v)	Sodium bicarbonate (w/v)	
B1	3	2	1	2	Chitosan cross-linking and uncontrolled gelation process resulting in inhomogeneous structure
B2	2	2	1	2	Chitosan cross-linking and uncontrolled gelation process resulting in inhomogeneous structure
B3	2	2	0.5	2	Chitosan cross-linking and uncontrolled gelation process resulting in inhomogeneous structure
B4	2	2	1	1	Homogeneous structure

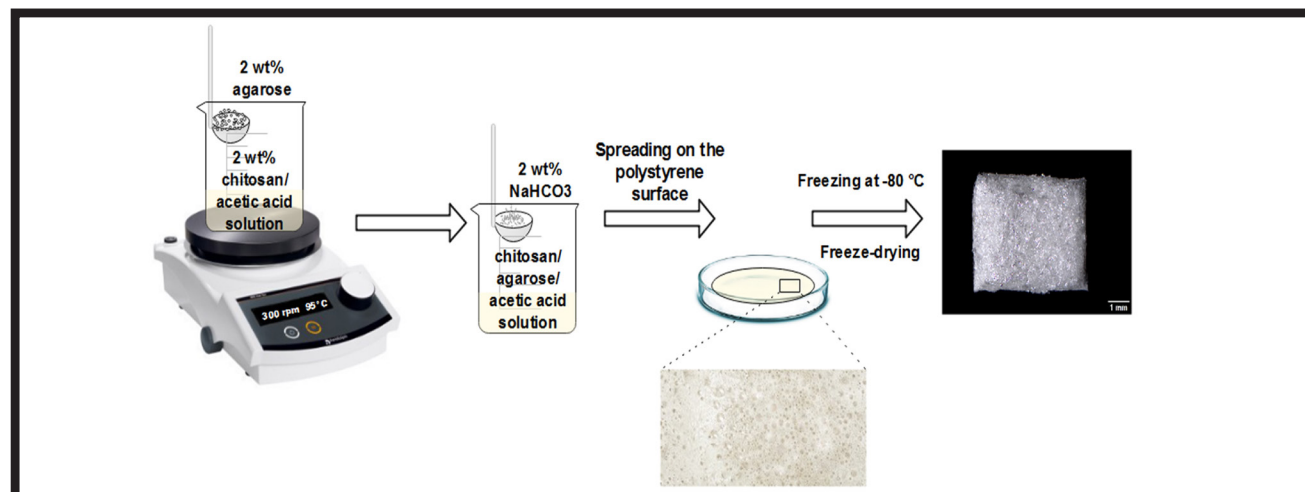


**FIG. 1. Schematic representation of the preparation process of chitosan/agarose-based biomaterials.**

### Cell culture

Normal human skin fibroblasts (BJ cell line) used in this study were bought from ATCC. The line was drawn from skin taken from normal foreskin. The cells were cultured in flasks using Eagle's Minimum Essential Medium supplemented with 10% foetal bovine serum, streptomycin (100 U/ml) and penicillin (100U/ml) to obtain a complete culture medium. The parameters of the culture conditions were as follows: 37°C, 5% CO<sub>2</sub> and 95% of air humidity. The cells were cultured for a period sufficient to approx. 90% confluency and then sub-cultured to obtain a sufficient number of cells. The BJ fibroblasts from the passages 4 -6 were used in the experiments.

### Cytotoxicity test using MTT assay

The *in vitro* cytotoxicity test was carried out in accordance with ISO 10993-5 standard using the fluid extracts of the materials. Briefly, the produced biomaterials were weighed and immersed in the EMEM culture medium at the ratio: 100 mg of the sample per 1 ml of the medium. To obtain the extracts the biomaterials were incubated for 24 h at 37°C. The polypropylene extract served as a negative control of cytotoxicity. To assess the cytotoxicity of the prepared biomaterials, the BJ cells were seeded in a 96-multiwell plate in 100 µl of EMEM at the concentration of  $2 \times 10^5$  cells/well. After the 24-hour incubation, the culture medium was replaced with 100 µl of the prepared extracts and the plates were left in an incubator for further 24 hours. Afterwards, the extracts were removed from the wells and 100 µl of 1mg/ml MTT solution was added to each well. The cells were incubated with MTT for 3 h at 37°C and the 0.01% (w/v) sodium dodecyl sulphate solution prepared in 0.01 M HCl was added to lyse the cells and dissolve the insoluble formazan. The absorbance of the obtained solution was measured at 570 nm using the microplate reader (BioTek Synergy H4 Hybrid).

### Cell viability determination by fluorescent technique

The non-toxic biomaterial (B4) selected in the MTT assay was subjected to the cytotoxicity evaluation based on fluorescent staining. The B4 I samples (5 mm x 5mm) were placed in the wells of a 48-multiwell plate and preincubated in the complete culture medium for 24 h. Then, 0.5 ml of the fibroblast suspension with the final concentration of  $2 \times 10^5$  cells/ml was seeded on the biomaterials and incubated for 2 days at 37°C. The BJ cells were grown for 2 days at the surface of the biomaterials and stained with the Live/Dead Cell Double Staining Kit according to the manufacturer instructions, using two reagents: calcein-AM and propidium iodide. Calcein-AM is a fluorescent dye that penetrates through the cellular membrane into cells, and during the test intracellular esterases present in the live cells remove the acetomethoxy group from the calcein, giving green fluorescence. Propidium iodide is used to stain dead cells. It is not membrane-permeable so it cannot penetrate healthy cells. The effect of live-dead reagents on the cell cultures was analyzed for green and red fluorescence using the confocal laser scanning microscope (Olympus Fluoview equipped with FV1000). The dead cells became visible as red ones while the viable fibroblasts - green.

### Statistical analysis

The MTT assay was repeated in 3 independent experiments and the obtained data were presented as the mean values  $\pm$  standard deviation (SD). The differences regarding cell viability of the tested samples were considered statistically significant at  $P < 0.05$ . All the statistical calculations were performed with the GraphPad Prism 6.0.0 software. The One-way Anova followed by the Tukey's test was used to determine statistical differences by comparing the tested groups.

## Results and Discussions

Structural and physicochemical characteristics of the biomaterial (e.g. porosity regarding pore size distribution, pore interconnectivity, pore volume and average pore size, surface chemical composition, wettability) is the key factor that must be considered while developing a new production method. The interconnected porous structure of biomaterials is required for the tissue ingrowth, cell penetration, waste and nutrient transport [18]. The highly porous structure is crucial for the material designed to act as a scaffold for skin cells (fibroblasts or keratinocytes). High porosity makes the biomaterials also more absorbent, which is a highly required property of the dressings to treat exudative wounds.

The foam-like structure of biomaterials was obtained by adding the gas foaming agent and applying the freeze-drying process (FIG. 2). The concentration of sodium bicarbonate (the gas foaming agent) used during the sample fabrication determined the amount of CO<sub>2</sub> gas release, which in turn resulted in the different porosity values of the resultant biomaterials. However, at the stage of adding sodium bicarbonate, the chitosan cross-linking and its gelation forming aggregates was noticed for the B1, B2, and B3 samples. This phenomenon resulted in their inhomogenous structure. It is known that a stable and firm gel is formed by neutralizing acidic chitosan solutions [19]. Thus, it was inferred that the excessive amount of sodium bicarbonate applied during the fabrication process caused the chitosan component gelation, due to the pH decrease. Among all the produced samples, only the B4 material, which was produced using the 1:1 ratio of the solvent and the gas-foaming agent, was characterized by the uniform and homogeneous structure (FIG. 2).

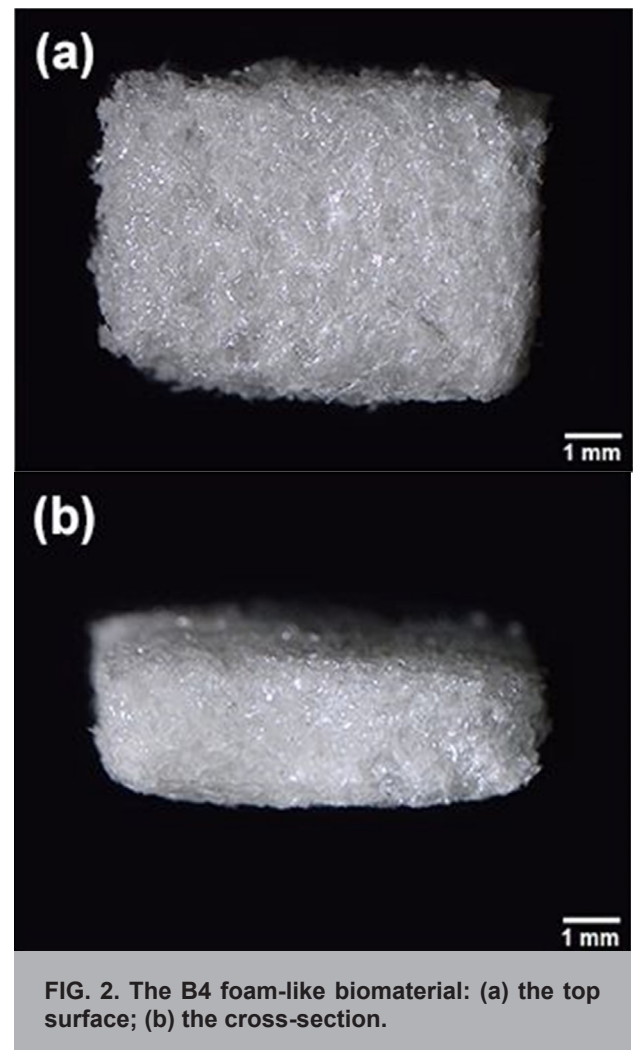


FIG. 2. The B4 foam-like biomaterial: (a) the top surface; (b) the cross-section.



The production method described in this work is unique because the individual components (chitosan, agarose), the gas foaming agent (sodium bicarbonate) and the solvent (acetic acid) were applied at concentrations that enabled the neutralization of the acidic chitosan solution. It was also possible to maintain the homogeneous structure without any traces of the chitosan precipitation or gelation. According to the available literature, other biomaterials based on agarose and chitosan were produced using two main approaches: the pH neutralization after the production process [20], or the production without the neutralization, which probably made the biomaterials toxic to the cells [21].

In this study, it was hypothesized that employing the foaming reaction and lyophilization may increase the specific surface area and the porosity of the resultant materials. The described method also enhances the material absorption capacity which is necessary to remove exudates from the wound. Nevertheless, future studies (e.g. the porosity liquid retention ability tests) need to be performed to confirm this assumption.

The conducted MTT assay showed that among all the tested biomaterials produced applying different concentrations of the components, only the B4 material was non-toxic to human skin fibroblasts (FIG. 3). Namely, although the chemical composition of all samples was the same, only the B4 biomaterial did not reduce cell viability. The B1-B3 biomaterials were characterized by the cell viability reduced to 8-11% as compared to the non-toxic polypropylene control. The viability of the fibroblast cell line exposed to the extract of the B4 material exceeded 92%. Cytotoxicity of the B1-3 samples may be explained by the excess of sodium bicarbonate in their structure which caused a pH significant increase the culture medium, exerting a lethal effect. According to the ISO standard, the biomaterial shall be considered non-toxic to the cells if the relative cell viability is over 70%, as compared to the control sample [22].

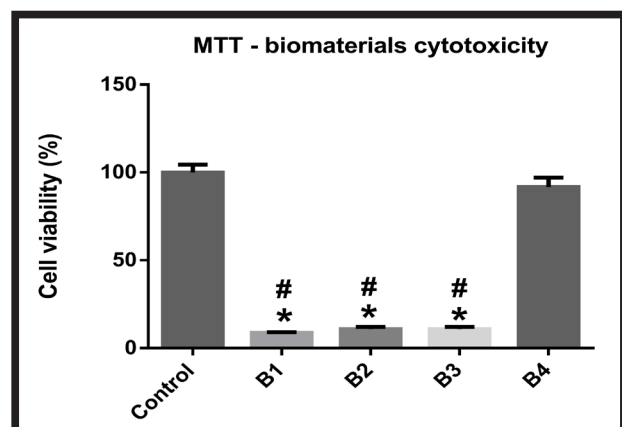


FIG. 3. Comparison of human fibroblasts viability after exposure to the extracts of the produced biomaterials based on the MTT assay; \*statistically significant differences compared to the control (cells exposed to polypropylene extract), #statistically significant differences compared to the B4 material,  $P < 0.05$ , One-way Anova followed by Tukey's test.

Since the B4 biomaterial revealed both the optimal foam-like structure (FIG. 2) and non-toxicity against skin fibroblasts, it underwent the cytotoxicity test based on the live-dead fluorescent assay. The confocal microscope observation confirmed its non-toxicity against BJ cells (FIG. 4a and b). A monolayer of viable (green fluorescence) and well flattened cells with normal fibroblastic morphology were visible around the biomaterial (FIG. 4c and d) and no flattened fibroblasts were noticed on the top surface (FIG. 4a). The human fibroblasts seeded on the biomaterial were viable and showed green fluorescence. Still they were round and not attached to the sample surface, which may indicate that the B4 biomaterial did not support the attachment of adherent cells, despite its lack of toxicity. In addition, no dead cells stained with red were observed, confirming the high biocompatibility of the B4 sample.

The tested biomaterial can be potentially used as an external wound dressing providing the barrier function between the wound and the external environment. Moreover, due to its foam-like structure, it reveals the high absorption ability, which will remove the wound exudates [23]. Since the B4 biomaterial was proved to be non-toxic and unfavourable to the fibroblast adhesion, it may act as a promising temporary dressing to cover the wound. What is more, after the treatment it can be removed without causing trauma to the wound bed.

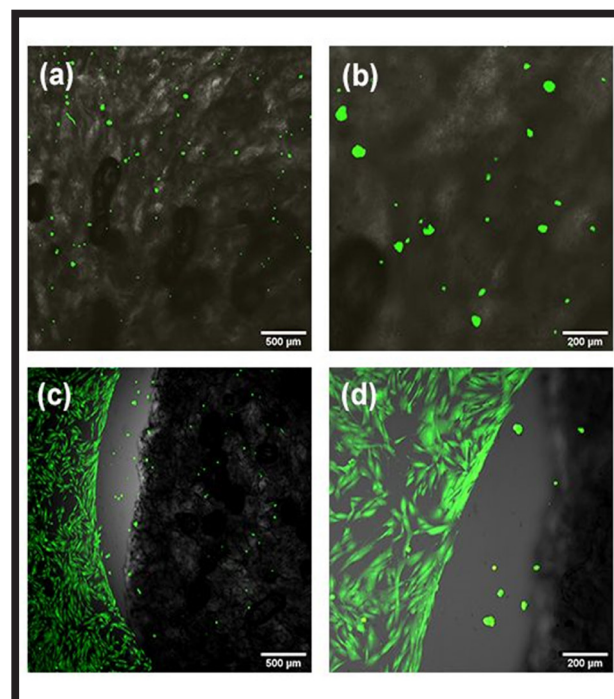


FIG. 4. Qualitative cytotoxicity evaluation of the B4 biomaterial: (a) and (b) live-dead staining of BJ cells grown directly on the biomaterial; (c) and (d) human fibroblasts cultured on the polystyrene next to the B4 biomaterial (merged images with green fluorescence – viable cells, red fluorescence – dead cells, Nomarski contrast highlights biomaterial structure).





## Conclusions

The presented study demonstrated that adding sodium bicarbonate to the chitosan/agarose mixture prepared in acetic acid allows obtaining the foam-like structure of the resultant biomaterial. It was proved that the material is non-toxic when sodium bicarbonate and acidic acid are applied at the 1:1 ratio. The biomaterial with the most promising biomedical potential was produced using 2% w/v chitosan, 2% w/v agarose, 1% v/v CH<sub>3</sub>COOH and 1% NaHCO<sub>3</sub>. The described here production method, involving the chitosan and agarose dissolution in acetic acid and the use of the foaming agent, may be potentially applicable for fabricating foam-like skin wound dressings. The biomaterial developed via this method is non-toxic and at the same time its surface does not support cell adhesion. Therefore, the biggest advantage of this biomaterial will be the painless removal of wound dressings after the successful healing process. Nevertheless, to fully confirm the biomedical potential of the developed material, the further detailed analysis regarding its mechanical, antibacterial, and biodegradable properties is recommended.

## Acknowledgments

The study was supported by the National Science Centre (NCN) in Poland within OPUS 16 grant no. UMO-2018/31/B/ST8/00945 and by using the equipment purchased within agreement no. POPW.01.03.00-06-010/09-00 Operational Program Development of Eastern Poland 2007-2013, Priority Axis I, Modern Economy, Operations 1.3. Innovations Promotion.




### ORCID iDs

V. Vivcharenko:  <https://orcid.org/0000-0002-1526-686X>  
 P. Kazimierzczak:  <https://orcid.org/0000-0002-5893-7168>  
 M. Wójcik:  <https://orcid.org/0000-0002-1918-6912>  
 A. Przekora:  <https://orcid.org/0000-0002-6076-1309>

## References

- [1] Clark R.A.F., Ghosh K., Tonnesen M.G.: Tissue engineering for cutaneous wounds. *Journal of Investigative Dermatology* 127 (2007) 1018-1029.
- [2] Vig K. et al.: Advances in Skin Regeneration Using Tissue Engineering. *International Journal of Molecular Sciences* 18 (2017) 789.
- [3] Catalano E., Cochis A., Varoni E., Rimondini L., Azzimonti B.: Tissue-engineered skin substitutes: an overview. *Journal of Artificial Organs* 16 (2013) 397-403.
- [4] Larouche D. et al.: Improved Methods to Produce Tissue-Engineered Skin Substitutes Suitable for the Permanent Closure of Full-Thickness Skin Injuries. *BioResearch Open Access* 5 (2016) 320-329.
- [5] Langer R., Vacanti J.P.: Tissue engineering. *Journal of Cellular Biochemistry* 44 (1990) 227-256.
- [6] Dhandayuthapani B., Yoshida Y., Maekawa T., Kumar D.S.: Polymeric Scaffolds in Tissue Engineering Application: A Review. *International Journal of Polymer Science* 2011 (2011) 1-19.
- [7] Rheinwald J.G.: Human epidermal keratinocyte cell culture and xenograft systems: applications in the detection of potential chemical carcinogens and the study of epidermal transformation. *Progress in clinical and biological research* 298 (1989) 113-125.
- [8] Vig K. et al.: Advances in skin regeneration using tissue engineering. *International Journal of Molecular Sciences* 18 (2017) 789.
- [9] Keck M., Lumenta D.B., Kamolz L.P.: Skin Tissue Engineering in Dermal Replacements in General, Burn, and Plastic Surgery, Vienna. Springer Vienna (2013) 13-25.
- [10] Cornelius V.J., Majcen N., Snowden M.J., Mitchell J.C., Vincina B.: Preparation of smart wound dressings based on colloidal microgels and textile fibres. *Smart Materials* 6413 (2006) 64130X.
- [11] Bharambe S. V., Darekar A.B., Saudagar R.B.: Wound healing dressings and drug delivery systems: A review. *International Journal of Pharmacy and Technology* 5 (2013) 2764-2786.
- [12] Mogoşanu G.D., Popescu F.C., Busuioc C.J., Pârvănescu H., Lascăr I.: Natural products locally modulators of the cellular response: Therapeutic perspectives in skin burns. *Romanian Journal of Morphology and Embryology* 53 (2012) 249-262.
- [13] Guerra L., Dellambra E., Panacchia L., Paionni E.: Tissue Engineering for Damaged Surface and Lining Epithelia: Stem Cells, Current Clinical Applications, and Available Engineered Tissues. *Tissue Engineering Part B: Reviews* 15 (2009) 91-112.
- [14] Maitz M.F.: Applications of synthetic polymers in clinical medicine. *Biosurface and Biotechnology* 1 (2015) 161-176.
- [15] Zilberman M., Elsner J.J.: Antibiotic-eluting medical devices for various applications. *Journal of Controlled Release* 130 (2008) 202-215.
- [16] Atiyeh B.S., Hayek S.N., Gunn S.W.: New technologies for burn wound closure and healing - Review of the literature. *Burns* 31 (2005) 944-956.
- [17] Loh Q.L., Choong C., Oxon D., Hons M., Mimm C.: Three-Dimensional Scaffolds for Tissue Engineering Applications. *Tissue Engineering Part B* 19 (2013) 485-502.
- [18] Julie G., Shuichi M.: Collagen scaffolds for tissue engineering. *Biopolymers* 89 (2008) 338-344.
- [19] Xu Y., Han J., Lin H.: Fabrication and characterization of a self-crosslinking chitosan hydrogel under mild conditions without the use of strong bases. *Carbohydrate Polymers* 156 (2017) 372-379.
- [20] Merlin Rajesh Lal L.P., Suraishkumar G.K., Nair P.D.: Chitosan-agarose scaffolds supports chondrogenesis of Human Wharton's Jelly mesenchymal stem cells. *Journal of Biomedical Materials Research - Part A* 105 (2017) 1845-1855.
- [21] Felfel R.M., Gideon-Adeniyi M.J., Zakir Hossain K.M., Roberts G.A.F., Grant D.M.: Structural, mechanical and swelling characteristics of 3D scaffolds from chitosan-agarose blends. *Carbohydrate Polymers* 204 (2019) 59-67.
- [22] International Standard ISO 10993-5 Biologiczna ocena wyrobów medycznych – Część 5: Badania cytotoxyczności in vitro 2009.
- [23] Salerno A., Netti P.A.: Introduction to biomedical foams, publ. Woodhead Publishing Limited, Italy 2014.

# WPŁYW WARSTWY POŚREDNIEJ NA POŁĄCZENIE METAL-CERAMIKA

ZOFIA KULA<sup>1\*</sup> , ŁUKASZ KOŁODZIEJCZYK<sup>2</sup> ,  
HIERONIM SZYMANOWSKI<sup>2</sup> 

<sup>1</sup> UNIWERSYTET MEDYCZNY W ŁODZI,  
KATEDRA STOMATOLOGII ODTWÓRCZEJ,  
ZAKŁAD TECHNIK DENTYSTYCZNYCH,  
UL. POMORSKA 251, 92-213 ŁÓDŹ

<sup>2</sup> POLITECHNIKA ŁÓDZKA, WYDZIAŁ MECHANICZNY,  
INSTYTUT INŻYNIERII MATERIAŁOWEJ,  
UL. STEFANOWSKIEGO 1/15, 90-924 ŁÓDŹ

\*E-MAIL: ZOFIA.KULA@UMED.LODZ.PL

## Streszczenie

*Protezy stałe wykonane na podbudowie metalowej licowane ceramiką stanowią istotną część metod uzupełnienia braków zębowych, jakie są do dyspozycji w dziedzinie protetyki stomatologicznej. Korzystne wyniki leczenia z zastosowaniem protez stałych, wykonanych ze stopu metalu i/lub ceramiki zależą w dużym stopniu od starannie przeprowadzonej diagnostyki układu stomatognatycznego, a także od właściwego zaplanowania postępowania klinicznego i laboratoryjnego. Najlepsze wyniki można osiągnąć tylko wtedy, gdy wybrany materiał na protezę stałą, a także sposób opracowania zęba będą zgodne również z oczekiwaniami pacjenta. Mimo iż rozwiązania tego typu są znane od bardzo dawna, nadal cieszą się ogromną popularnością wśród pacjentów. Spowodowane jest to bardzo dobrą wytrzymałością oraz odpowiednią estetyką, która jest bardzo ważna dla pacjentów. Wysoką estetykę uzyskuje się poprzez licowanie konstrukcji podbudowy metalowej ceramiką tlenkową, która niemal identycznie odzwierciedla twarde tkanki zęba.*




*W pracy wykorzystano stopy firmy Dentaurum Remanium CSe, na których powierzchnię zostały nałożone warstwy opakerów w postaci proszku i pasty. Na powierzchnię stopu nałożono ceramikę firmy Vita Master oraz VM13. Próbkę zostały poddane badaniu chropowatości, porowatości oraz przeprowadzono analizę pierwiastków w danym obszarze ceramiki.*

*Przeprowadzone badania wykazują, że warstwa pośrednia (opakerowa) wpływa na połączenie stopu z ceramiką. Najlepsze rezultaty wykazuje gdy porowatość jest minimalna. Na podstawie wyników nie stwierdzono wpływu rodzaju warstwy pośredniej na wytrzymałość połączenia stopu z ceramiką. Potwierdzono, że parametr chropowatości istotnie wpływa na wytrzymałość połączenia metal-ceramika. Badania morfologiczne wykonane przy użyciu mikroskopu skaningowego SEM wykazały, że po wypaleniu zachodzą zmiany w stężeniu pierwiastków na granicy ceramika-stop.*

**Słowa kluczowe:** ceramika, metal, oksydacja, warstwa pośrednia

[Inżynieria Biomateriałów 152 (2019) 21-28]

# INFLUENCE OF THE INTER-MEDIATE LAYER ON THE METAL-CERAMICS BOND STRENGTH

ZOFIA KULA<sup>1\*</sup> , ŁUKASZ KOŁODZIEJCZYK<sup>2</sup> ,  
HIERONIM SZYMANOWSKI<sup>2</sup> 

<sup>1</sup> MEDICAL UNIVERSITY OF LODZ,  
CHAIR OF RESTORATIVE DENTISTRY,  
UL. POMORSKA 251, 92-213 ŁÓDŹ, POLAND

<sup>2</sup> LODZ UNIVERSITY OF TECHNOLOGY,  
FACULTY OF MECHANICAL ENGINEERING,  
INSTITUTE OF MATERIALS ENGINEERING,  
UL. STEFANOWSKIEGO 1/15, 90-924 ŁÓDŹ, POLAND

\*E-MAIL: ZOFIA.KULA@UMED.LODZ.PL

## Abstract

*Fixed alloy and ceramic prostheses constitute an important part of remedies available at the disposal of restorative dentistry. The successful treatment with fixed prostheses made of alloy or ceramics, or a combination of both materials, depends to a large extent on the thorough diagnosis of the masticatory organ, as well as the proper planning of clinical and laboratory procedures. The best results can only be achieved if the material chosen for the permanent prosthesis and the method of developing the tooth is also adjusted to the patient's expectations. Although this type of solution has been known for a very long time, it is still very popular among patients. This is due to very good durability and appropriate aesthetics, which is very important for patients. High aesthetics is achieved by veneering the metal framework construction with oxide ceramics that almost identically reflect the hard tooth tissues.*

*In this work, we used the Remanium CSe alloy with layers of powder and paste applied to the surface. The samples were subjected to the roughness, porosity, as well as elemental analysis in a given area of ceramics.*

*The conducted examinations showed that the intermediate (opaque) layer affects the connection of the alloy with ceramics. The best results were achieved when the porosity was minimal. Based on the results of the study, it was found that the type of intermediate layer did not influence the strength of the alloy with ceramics. It was confirmed that the roughness parameter significantly affected the strength of the metal-ceramic bond. Morphological studies via SEM scanning microscopy showed that after firing, changes occurred in the concentration of elements at the ceramic-alloy border.*

**Keywords:** alloy, ceramics, oxidation, intermediate layer

[Engineering of Biomaterials 152 (2019) 21-28]



Mimo coraz nowocześniejszych technik, urządzeń i materiałów służących do wykonania stałych uzupełnień protetycznych, technika metalowo-ceramiczna wciąż pozostaje niezawodną i popularną metodą wykonania różnego rodzaju prac protetycznych (korony, mosty).

Połączenie pomiędzy metalem a ceramiką uzyskuje się na drodze chemicznej, fizycznej i mechanicznej [1]. Połączenie chemiczne w tym przypadku to reakcje zachodzące pomiędzy warstwą tlenków, a masą opakera. Siła występujących wiązań chemicznych nie jest zbyt duża, dlatego należy szczególnie dokładnie przygotować powierzchnię metalu, aby uzyskać trwałe połączenie stopu z ceramiką [2,3].

Aby zwiększyć adhezję ceramiki do podbudowy, należy odpowiednio dopasować współczynnik rozszerzalności cieplnej między podbudową a ceramiką. Dobre połączenie między metalem a ceramiką wymaga doboru materiałów o odpowiednich współczynnikach rozszerzalności cieplnej. Współczynnik rozszerzalności cieplnej ceramiki jest tylko nieznacznie mniejszy niż metalu [4]. W celu uzyskania odpowiedniego połączenia różnica ta powinna wynosić pomiędzy  $0,5-1,5 \times 10^{-6}/K$  w temperaturze 25-500°C. Współczynnik podbudowy metalowej, jak i ceramicznej powinien mieć niższą wartość. Jest to związane ze skurczem ceramiki [5]. W większości przypadków producenci ceramiki podają tabele stopów, na których można napalać daną ceramikę. Trzeba też przyjąć, że jeśli różnica we współczynnikach rozszerzalności cieplnej jest mała, konstrukcję należy studzić szybciej. Postępowanie to jest związane z naprężeniami powstającymi na styku ceramiki i podbudowy. Przy szybkim studzeniu może dojść do powstania pęknięć materiału ceramicznego [4,6-8].

W celu zwiększenia rozwinięcia powierzchni wykorzystuje się piaskowanie, które może przyczynić się do lepszego połączenia stopu z ceramiką. Powierzchnia uzyskuje wtedy większą chropowatość. Istotne też jest użycie rodzaju i wielkości ścierniwa.

Jakość połączenia metalowo-ceramicznego zależy od działania kilku czynników: zwilżalności porcelany, grubości warstwy tlenkowej, połączenia mechanicznego, połączenia związanego z różnicą kurczliwości materiałów, dyfuzji [8]. Dobre zwilżenie powoduje głęboką penetrację ceramiki w strukturę metalu. Proces zwilżenia, który jest bardzo ważny dla dobrego połączenia metal-ceramika może zostać zaburzony przez zanieczyszczenia. Jedną z metod czyszczenia powierzchni metalowych jest używanie pary wodnej. Po tej czynności struktura metalowa nie powinna być dotykana [9].

Grubość warstwy tlenków ma wpływ na adhezję między stopem a ceramiką. Nie może być zbyt gruba ani zbyt cienka [9]. W warstwie tej następuje dyfuzja atomów z powierzchni stopu i ceramiki oraz powstaje między atomami zawartymi w stopie i tlenie – czyli powstania tlenków. Pozostawiona warstwa polepsza ostateczne właściwości mechaniczne [9].

Celem niniejszej pracy było określenie wpływu warstwy połączenia metal-ceramika. Część badawcza obejmuje badania porowatości, a także określenie zawartości pierwiastków w poszczególnych warstwach przy pomocy mikroskopu skaningowego.

Despite the development of more and more modern techniques, equipment and materials used to manufacture permanent prosthetic restorations, the metal-ceramic method is still a dominant one to perform various types of prosthetic work due to its reliability and predictability.

The connection between metal and ceramics is obtained chemically, physically and mechanically [1]. The chemical bond results from the reaction between the oxide layer and the intermediate layer connecting the alloy to the ceramic. The strength of the occurring chemical bonds is not particularly high, so it is important to prepare the metal surface carefully to obtain the permanent bonding of the ceramic alloy [2,3].

In order to increase the forces that cause adhesion, the thermal expansion coefficients between the support and the ceramics should be appropriately chosen. A good connection between metal and ceramics requires the selection of materials with appropriate thermal expansion coefficients. The thermal expansion coefficient of the ceramics is only slightly lower than the one of metal [4]. To assure adequate adhesion, the difference should be between  $0.5-1.5 \times 10^{-6}/K$  at 25-500°C. Both the metal and the ceramics substructures should be endowed with lower values since after cooling the ceramics is pressed against the metal surface as a result of the difference in the thermal expansion parameters [5]. In most cases, the ceramics manufacturers provide tables of alloys that can be fired on particular ceramics. It is also important to assume that if the difference in thermal expansion coefficients is small, the structure should be cooled faster. This procedure is related to the pressures arising at the contact of the ceramic underlay. During the rapid cooling process, cracks in the ceramic material might occur [4,6-8].

In order to facilitate surface development, the sandblasting technique is used, which can contribute to the better connection between the alloy and ceramics.

The quality of the metal-ceramics joints that occur during permanent prosthetic work is a result of several factors, such as ceramics wetting, oxide layer thickness, mechanical joint, shrinkage difference, diffusion. The efficient wetting causes deep penetration of the ceramics into the irregular metal structure. However, the moisturizing process, which is very important for a good metal-ceramics combination can be inhibited by impurities. One of the methods of cleaning metal surfaces is water vapor. After this process, the metal structure should not be touched [9].

The thickness of the oxide layer affects the adhesion between the alloy and the ceramics. It should not be either too thick or too thin. In this layer two processes take place: the diffusion of atoms from the alloy surface and the ceramics and the formation of the oxide between the alloy atoms and oxygen. The obtained layer improves the final properties of the joint.

The purpose of this work was to determine the effect of the metal-ceramic joint layer. The research part includes porosity tests, as well as determining the content of elements in individual layers, using a scanning microscope.

## Materialy i metody

Zakres pracy obejmuje ocenę połączenia ceramiki ze stopem nikiel-chrom na podstawie wykonanych próbek przy użyciu trzech warstw pośrednich: w formie proszku drobnopowidelnego do stosowania w konwencjonalnym zakresie WRC (próbka A), w postaci proszku do stosowania w zakresie WRC 13,8-15,2 (próbka C) oraz konsystencji pasty (próbka B). W pracy użyto ceramiki tlenkowej firmy Vita. Ceramika ta zawiera SiO<sub>2</sub> 58-63%, Al<sub>2</sub>O<sub>3</sub> 20-23%, Na<sub>2</sub>O 6-11%, K<sub>2</sub>O 4-6%, B<sub>2</sub>O<sub>3</sub> 0,5-2% CaO <1% i TiO<sub>2</sub> <1%. W TABELI 1 przedstawiano poszczególne próbki z różnymi warstwami pośrednimi.

**TABELA 1. Próbkę przeznaczony do badań.**  
**TABLE 1. Description of individual samples.**

Próbka A Sample A	Opaker + ceramika Intermediate layer + final ceramics
Próbka B Sample B	Opaker w formie pasty + ceramika Intermediate layer in the form of paste + final ceramics
Próbka C Sample C	Wash Opaker + opaker + opakdentyna + ceramika 2 <sup>nd</sup> intermediate layer + additional bonding layer + specific ceramics

Próbki przeznaczony do badań zostały wykonane ze stopu Rermanium CSe NiCrMo o średnicy 0,5 mm. W skład tego stopu wchodzi Ni 61%, Cr 26%, Mo 11%, Si 1,5% i Fe 1,2%. Na ich powierzchnię zostały nałożony warstwy opakera w postaci proszku i pasty. Do badań użyto po 3 próbki z każdego rodzaju. Próbki stopu nikiel-chrom zostały przeszlifowane na papierach o ziarnistości 800 i 1200, aby uzyskać gładką, oczyszczoną powierzchnię. Kolejnym etapem było wypiskowanie próbek tlenkiem glinu o rozmiarze ziarna 110 µm pod ciśnieniem 2,5 bara, które miało na celu rozwinięcie powierzchni, a tym samym zwiększenie przyczepności nakładanej ceramiki. Przed przystąpieniem do nakładania opakera każda z próbek została oczyszczona pod ciśnieniem pary wodnej. Procedura nakładania ceramiki na powierzchnię metalu była zgodna z zaleceniem producenta. Pierwszym etapem jest nakładanie opakera, który nadaje koronie podstawowy odcień. Opaker w proszku jest rozrabiany z płynem VITA VM OPAQUE FLUID. Masa powinna mieć wodnistą konsystencją. Za pomocą pędzla nakłada się opaker na suchą i czystą strukturę metalową. Następnie pokrywa się powierzchnię licowaną rozrobionym opakera za pomocą pędzla lub szpatełki i napala się. Analogicznie pokrywa się suchą strukturę metalową opakera w paście. Po nałożeniu dentyny, nakłada się warstwę masy VITAVM.13 ENAMEL. Po nałożeniu każdej z warstw ceramika była napalana w piecu do ceramiki firmy Vita. Temperatura wypalania ceramiki to 890-960°C.

Badania profilometryczne wykonano z wykorzystaniem konfokalnego laserowego mikroskopu skaningowego (CLSM) Nikon MA200. Jest to mikroskop uniwersalny o odwróconej optyce, który wyposażony został w najnowszy system konfokalny C1. System C1 umożliwił obserwację i rejestrację przekrojów optycznych badanych próbek, które posłużyły do analizy topografii powierzchni. Źródłem światła w mikroskopie konfokalnym są lasery, które posiadają wiązkę światła o określonej długości fali i natężeniu. Do skanowania powierzchni próbek wykorzystano laser argonowy o długości fali  $\lambda = 488$  nm. Obrazy rejestrowano przy pomocy programu EZ-C1. Obrazy z mikroskopii optycznej zostały opracowane w programie ImageJ, który został specjalnie dostosowany do mikroskopu w celu uzyskania informacji odnośnie porowatości. Do analizy przekroju warstw ceramiki posłużył mikroskop metalograficzny.

## Materials and Methods

The scope of this work includes evaluating the combinations of nickel-chromium alloy and ceramics. Three types of intermediate layers were used: fine powder in the conventional WRC range (sample A), powder for WRC 13.8-15.2 (sample C) and paste (sample B). Vita oxide ceramics was used in the work. These ceramics contains SiO<sub>2</sub> 58-63%, Al<sub>2</sub>O<sub>3</sub> 20-23%, Na<sub>2</sub>O 6-11%, K<sub>2</sub>O 4-6%, B<sub>2</sub>O<sub>3</sub> 0.5-2% CaO <1% and TiO<sub>2</sub> <1%. TABLE 1 shows individual samples with different intermediate layers.

The test samples were made of 0.5 mm diameter Rermanium CSe NiCrMo alloy. This alloy consists of Ni 61%, Cr 26%, Mo 11%, Si 1.5% and Fe 1.2%. On their surface, opaque layers were applied in the form of powder and paste. The nickel-chromium alloy samples were ground on 800 and 1200 grain papers to obtain a smooth and clean surface. Next, the samples were sandblasted with the aluminum oxide powder of 110 µm in diameter at the 2.5 bar pressure to develop their surface and thus increase the adhesion of the applied ceramics. Before applying the first layer of ceramics (intermediate layer), all samples were cleaned under the steam pressure. The procedure for applying ceramics to the metal surface stayed in accordance with the manufacturer's instructions. The first stage was the application of opaque, which gives the crown a basic shade. The powder opaque was mixed with VITA VM OPAQUE FLUID. The mass should have a watery consistency. The opaque was applied to a dry and clean metal structure with a brush. Then the veneered surface was covered with the crushed opaque with a brush or spatula and fired on. Similarly, the dry metal structure was coated with the opaque paste. After applying dentin, a layer of VITAVM.13 ENAMEL was applied. After applying each layer, the ceramics were fired in a Vita ceramic oven. The ceramic firing temperature was 890-960°C.

The profilometric tests were performed using Nikon MA200 confocal laser scanning microscope (CLSM) with inverted optics equipped with the latest confocal C1 system. The C1 system allowed for the observation and recording of the optical cross-sections of the samples to analyze the surface topography. An argon laser wavelength  $\lambda = 488$  nm was used to scan the surface of the samples. The images were recorded using the EZ-C1 program. The resolution of the recorded images was 512×512 pixels. A detailed analysis of the confocal microscope data was performed using the MountainsMap Premium program. The calculations were performed in east-west direction.

Do oceny powierzchni połączenia wykorzystano dodatkowo elektronowy mikroskop skaningowy JEOL JSM – 6610LV przy pomocy standardowego oprogramowania. Napięcie przyspieszające wynosiło 20 kV. Rozdzielczość rejestrowanych obrazów wynosiła 512×512 pikseli. Szczegółowa analiza danych uzyskanych za pomocą mikroskopu konfokalnego została przeprowadzona przy pomocy programu MountainsMap Premium firmy Digital Surf. Obliczenia dotyczyły odcinka skierowanego w kierunku wschód-zachód. W celu określenia zawartości pierwiastków w poszczególnych obszarach wykonano mikroanalizę rentgenowską (EDS) firmy NORAN z oprogramowaniem VENTAGE oraz wykonano identyfikację faz metodą dyfrakcji elektronów wstecznie rozproszonych EBSD firmy NORAN.

Obrazy uzyskane za pomocą mikroskopu optycznego metalograficznego zinterpretowano przy użyciu programu ImageJ w celu określenia porowatości danej próbki. Wymagało to przetworzenia otrzymanych zdjęć na obrazy 8 bitowe w skali szarości oraz zwiększeniu kontrastu w celu zróżnicowania detali.

Następnie wykonano badanie przy użyciu elektronowego mikroskopu skaningowego HITACHI S-3000N, wyposażonego w zestaw do mikroanalizy rentgenowskiej (EDS-NORAN). Badania wykonano w celu określenia zawartości pierwiastków w poszczególnych obszarach ceramiki.

## Wyniki i dyskusja

Na RYS. 1 przedstawiono strukturę geometryczną powierzchni badanych próbek po piaskowaniu. Dane te otrzymane zostały za pomocą mikroskopu konfokalnego CLSM.

Na RYS. 2 znajdują się struktury geometryczne powierzchni badanych próbek po wypaleniu.

TABELA 2 zawiera wartości parametrów chropowatości.

Na podstawie wyników widać zmianę chropowatości powierzchni próbek objawiającą się w zwiększeniu wartości Ra, Rz oraz Rq po wypaleniu. Największe różnice wykazują powierzchnie próbki A i B. Największą wartością współczynnika Ra charakteryzowała się próbka C. Parametr chropowatości w przypadku połączenia metalu z ceramiką ma szczególne znaczenie. Im większy jest ten parametr, tym większa jest możliwość uzyskania lepszego połączenia metalu z ceramiką.

RYS. 3 przedstawia morfologię zastosowanych w pracy warstw pośrednich w formie proszku. Oba materiały charakteryzują się bardzo podobną morfologią.

Ocenę porowatości poszczególnych próbek dokonano na podstawie obrazów metalograficznych badanych powierzchni, które zamieszczono w TABELI 3. Badania jednoznacznie wskazują na większą porowatość ceramiki w postaci proszku do stosowania w zakresie WRC 13,8-15,2.

W celu określenia zawartości pierwiastków w poszczególnych obszarach ceramiki wykonano analizę za pomocą elektronowego mikroskopu skaningowego. Obszary analizy ceramiki przedstawiono na RYS. 4. Rysunek został podzielony na 5 obszarów. Obszar od 1 do 3 to obszar ceramiki właściwej, obszar 4 to warstwa pośrednia czyli opakierowa, natomiast obszar 5 to powierzchnia metalu.

The metallographic microscope was used to analyze the cross-sections of the ceramics in order to obtain the porosity values. The images from optical microscopy were processed using ImageJ program, which required transforming them into grayscale 8-bit images and increasing the contrast to differentiate the details.

The HITACHI S-3000N scanning electron microscope, equipped with NORAN's X-ray microarrays (EDS) with VENTAGE software and the NORAN-based EBSD EBSD diffraction kit, were used to determine the content of elements in individual ceramic areas.

## Results and Discussion

FIG. 1 represent the geometric surface structure of the sandblasted samples. The data was obtained by means of the CLSM confocal microscope.

FIG. 2 represent the geometric sample structure after stoving.

The TABLE 2 shows the roughness parameters results.

Based on the results, it can be observed that the surface roughness parameters Ra, Rz, and Rq values increased after stoving. The biggest differences were noticed for the samples A and B. The sample C was characterized by the highest Ra value.

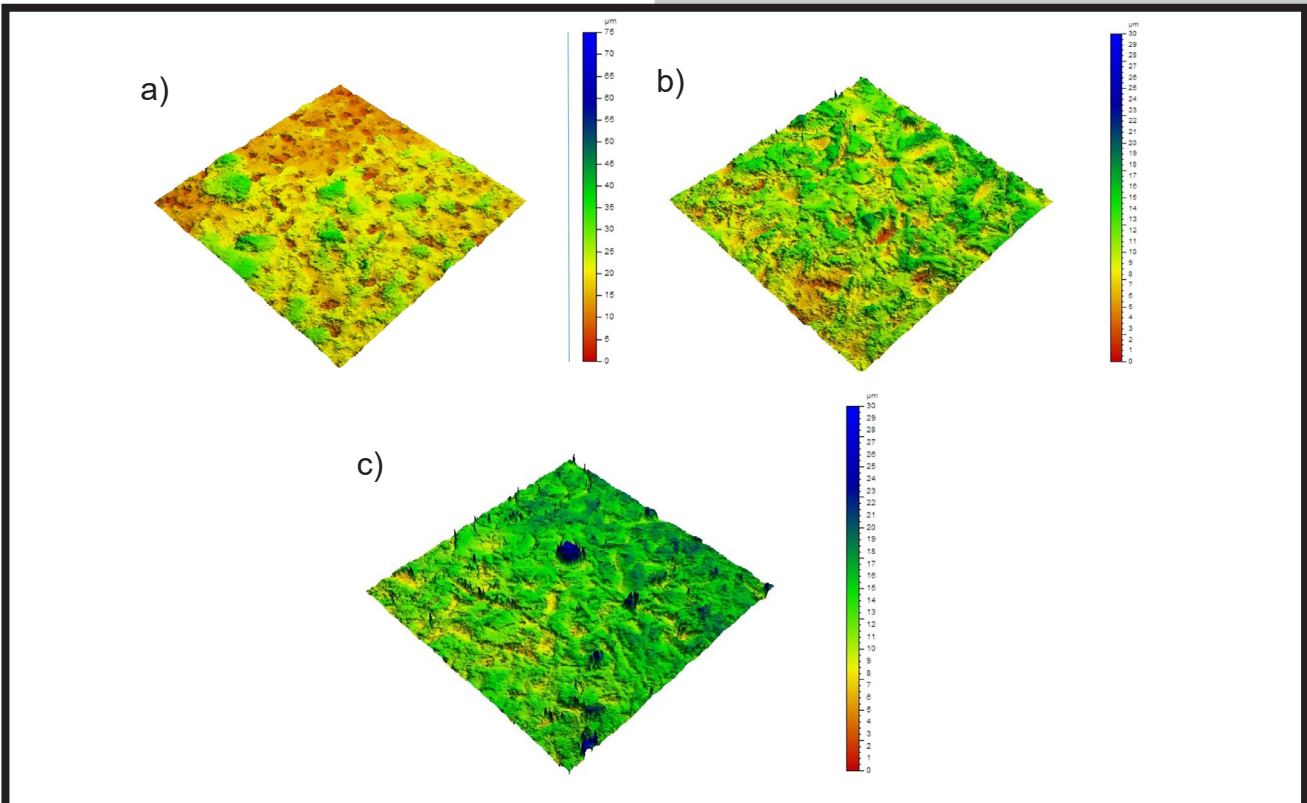
The morphologies of the powder intermediate layers are depicted in FIG. 3. The image shows that both powders have very similar morphologies.

The porosity evaluation of individual samples was conducted on the basis of metallographic images of the examined surfaces. The TABLE 3 represents the results showing that the sample C is characterized by the largest porosity.

The tests clearly indicated the higher porosity of the powder ceramics used in the WRC 13.8-15.2 range. In order to determine the content of elements in particular areas of the ceramics, the SEM analysis was performed. The areas of ceramics analysis are shown in FIG. 4.

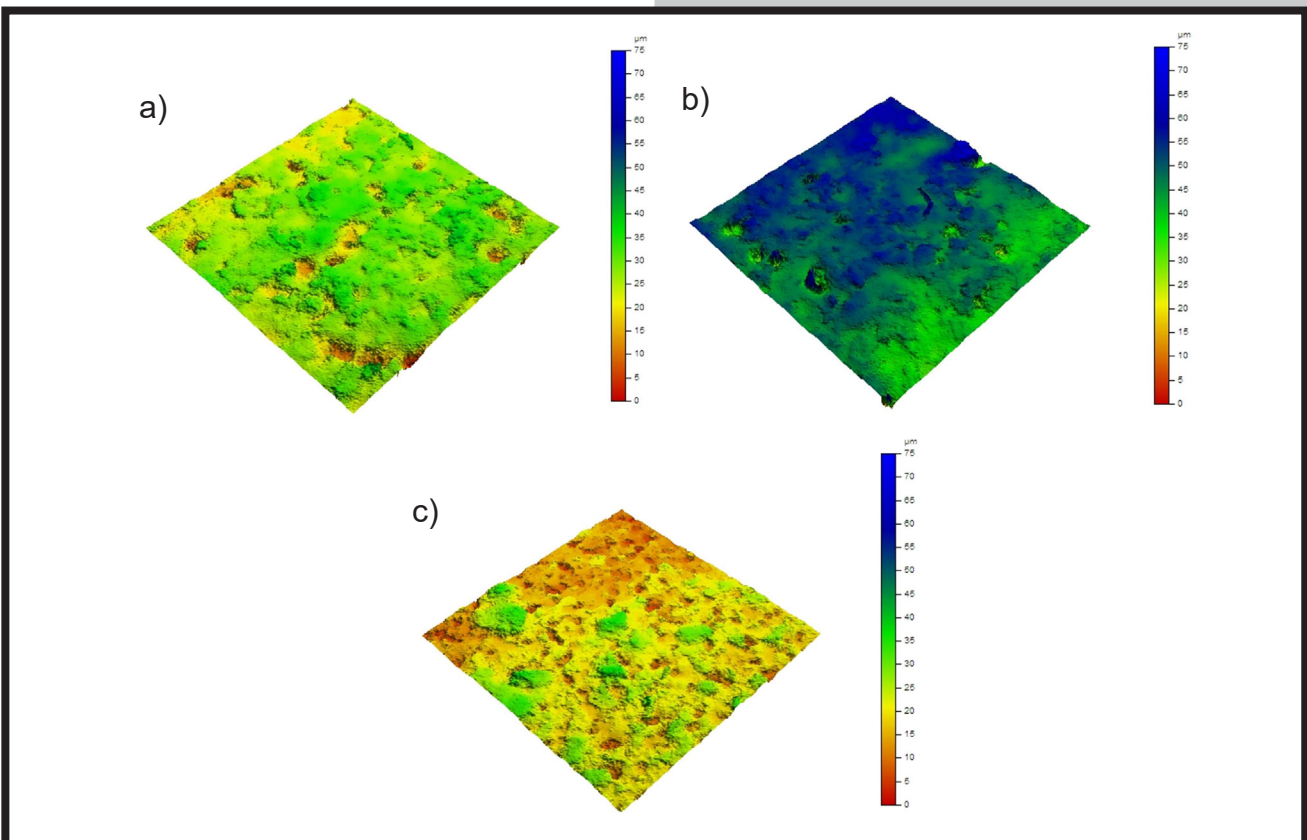
The TABLE 4 shows the content of elements in each area of ceramics after stoving.





RYS. 1. Struktura geometryczna powierzchni: a) próbka A po piaskowaniu, b) próbka B po piaskowaniu, c) próbka C po piaskowaniu.

FIG. 1. Geometric surface structure: a) sample A after sandblasting, b) sample B after sandblasting, c) sample C after sandblasting.

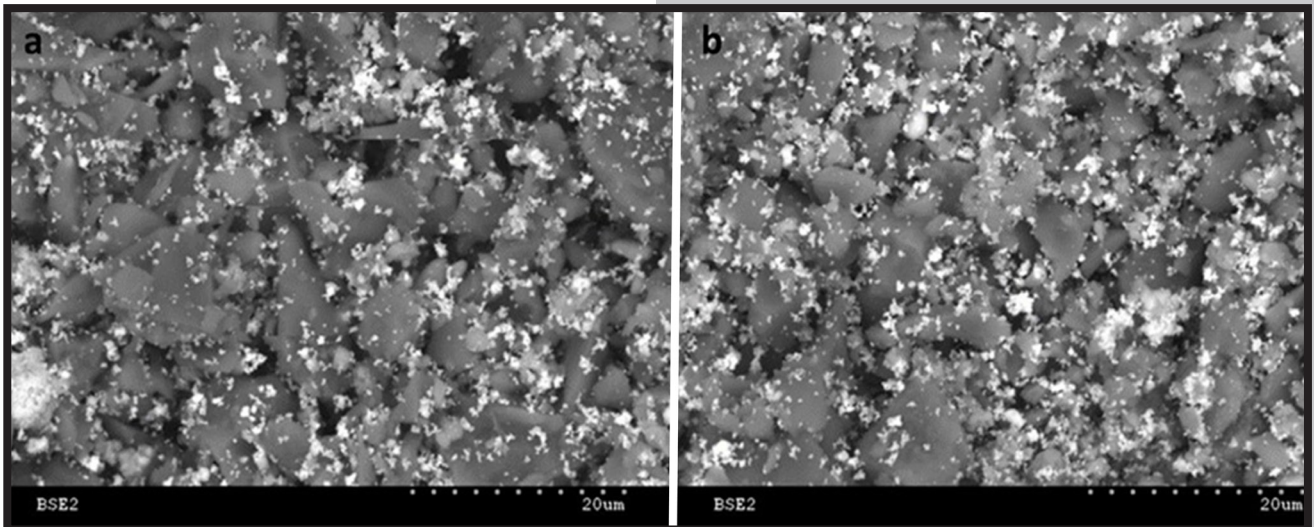


RYS. 2. Struktura geometryczna powierzchni: a) próbka A po wypaleniu, b) próbka B po wypaleniu, c) próbka C po wypaleniu.

FIG. 2. Geometric surface structure: a) sample A after firing, b) sample B after firing, c) sample C after firing.

TABELA 2. Zestawienie wyników parametrów chropowatości.  
TABLE 2. List of roughness parameters results.

Próbki Samples	Ra po wypaleniu Ra after stoving [ $\mu\text{m}$ ]	Ra po piaskowaniu Ra after sandblasting [ $\mu\text{m}$ ]	Rz po piaskowaniu Rz after sandblasting [ $\mu\text{m}$ ]	Rz po wypaleniu Rz after stoving [ $\mu\text{m}$ ]	Rq po piaskowaniu Rq after sandblasting [ $\mu\text{m}$ ]	Rq po wypaleniu Rq after stoving [ $\mu\text{m}$ ]
Próbka A Sample A	1.82	1.23	8.54	12.5	1.65	2.45
Próbka B Sample B	1.65	1.19	8.23	13.5	1.59	2.39
Próbka C Sample C	1.9	1.13	9.88	8.5	1.63	1.74



RYS. 3. Obrazy uzyskane za pomocą mikroskopu elektronowego z obserwacją elektronów wstecznie rozproszonych (BSE) przedstawiające morfologie opakerów: a) próbka A, b) próbka C.  
FIG. 3. SEM images (BSE mode) of the powders used as intermediate layers: a) sample A, b) sample C.

TABELA 3. Wyniki porowatości poszczególnych próbek.  
TABLE 3. Porosity values of individual samples.

Powiększenie Magnification	Próbka A Sample A	Próbka B Sample B	Próbka C Sample C
Powiększenie Magnification 100x	2.43%	1.62%	8.25%
Powiększenie Magnification 200x	2.23%	0.55%	10.6%
Powiększenie Magnification 300x	0.82%	0.58%	8.3%



RYS. 4. Analiza obszarów ceramiki.  
FIG. 4. Analysis of ceramic areas.

**TABELA 4. Zawartość pierwiastków w poszczególnych obszarach po wypaleniu ceramiki.**  
**TABLE 4. The content of elements in particular areas of ceramics after firing.**

Pierwiastki Elements	Obszar 1 Area 1 [%] at.	Obszar 2 Area 2 [%] at.	Obszar 3 Area 3 [%] at.	Obszar 4 Area 4 [%] at.	Obszar 5 Area 5 [%] at.
O	49.52	51.45	48.41	41.73	-
Na	4.73	5.31	5.08	3.78	-
Al	7.90	7.90	7.86	7.17	0.22
Si	27.45	27.08	28.23	21.27	3.16
Zr	1.01	0.85	0.97	3.94	-
K	6.21	5.56	6.67	6.19	-
Ca	0.84	0.64	1.04	0.85	-
Ti	1.14	0.69	0.99	5.26	-
Ce	1.19	0.53	0.74	9.82	-
Mo	-	-	-	-	3.27
Cr	-	-	-	-	22.60
Mn	-	-	-	-	1.44
Fe	-	-	-	-	42.38
Ni	-	-	-	-	26.93

W TABELI 4 przedstawiono zawartość pierwiastków w poszczególnych obszarach po wypaleniu ceramiki.

Badania te dowodzą, że po wypaleniu zachodzą zmiany w stężeniu pierwiastków na granicy ceramika-stop. Zawartość Zr, Ti i Ce zwiększa się, natomiast Si, O i Na zmniejsza się. Świadczy to o wystąpieniu dyfuzji w badanych obszarach.

Niewielka ilość Al i Si uległa dyfuzji do obszaru stopowego. Stwierdzono tam następujące zawartości: 0,22% at. dla Al i 3,16% at. dla Si. Zachodzi także utlenianie stopu. Procesy te prowadzą do powstania warstwy przejściowej, która w istotny sposób wpływa na wytrzymałość i szczelność złącza. W wyniku obróbki cieplnej, a w szczególności niezgodności współczynników rozszerzalności cieplnej ceramiki i warstwy metalicznej, powstają w układzie naprężenia wpływające na wytrzymałość połączenia.

Parametry chropowatości Ra, Rz i Rq zwiększyły się po wypaleniu w przypadku wszystkich badanych próbek. Z otrzymanych danych wynika, że wash opaker Vita VM13 ma największą chropowatość po wypaleniu, a najmniejszą opaker Vita VMK. Może to być spowodowane intensywnymi procesami utleniania warstwy wierzchniej badanych próbek w wysokich temperaturach ich wypalania (890-960°C). Wraz ze wzrostem chropowatości rośnie rozwinięcie powierzchni, co może skutkować wzrostem wytrzymałości połączenia.

Dzięki analizie obrazów EDS można stwierdzić, że warstwy pośrednie nie różnią się znacznie między sobą pod względem wielkości ziaren i składu chemicznego – analiza EDS. Producent ceramiki Vita twierdzi, że ziarna Vit-y VM13 są okrągłe i mają 18 µm. Natomiast w przypadku ceramiki Vita VMK Master ziarna wynoszą ok. 19 µm. Jednak z wykonanych badań wynika, iż obie ceramiki mają budowę ziaren płatkową. Mniejsze ziarna umożliwiają lepsze połączenie się ceramiki, a to mogło minimalnie polepszyć połączenie w przypadku Vita VM13 mimo, że różnica w wielkości między tymi ceramikami jest niewielka.

Dodatkowo badania morfologiczne wykonane przy użyciu mikroskopu skaningowego SEM wykazały, że po wypaleniu zachodzą zmiany w stężeniu pierwiastków na granicy ceramika-stop. Zawartość Zr, Ti i Ce zmniejsza się w kierunku poszczególnych warstw ceramiki. Świadczy to o wystąpieniu zjawiska dyfuzji w badanych obszarach w wyniku procesów dyfuzyjnych. Prawdopodobnie pierwiastek Si dyfundował do obszaru stopu, gdyż jego zawartość się zwiększyła porównując go ze składem przed wypaleniem.

These studies showed that the concentration of elements on the ceramics-alloy border-line changed after stoving. The content of Zr, Ti and Ce increased while the Si, O and Na amount was reduced. This proves the appearance of diffusion in the studied areas.

A small amount of Al and Si was diffused into the alloy area the contents were as follows: 0.22% at. for Al and 3.16% at. for Si. It also oxidized the alloy. These processes led to the formation of a transition layer which significantly affects the strength and tightness of the joint. As a result of the heat treatment, and in particular the incompatibility of the thermal expansion coefficients of the ceramics and the metallic layer, tensions build up in the system which affect the bond toughness.

The roughness parameters Ra, Rz, and Rq increased for all tested samples after firing. The obtained data showed that the wash opaque Vita VM13 had the highest roughness after firing, and the smallest opaque - Vita VMK. This phenomenon may result from the intensive oxidation of the surface layer at high firing temperatures (890-960°C). The surface development increases as the roughness increases, which can result in the increased bond strength.

Thanks to the analysis of EDS images, it can be concluded that the intermediate layers do not differ significantly in terms of the grain size and chemical composition. The ceramics manufacturer Vita claims that Vit-y VM13 grains are round and measure 18 µm. In the case of Vita VMK Master ceramics, the grains are about 19 µm. However, the research showed that both kinds of ceramics have a flake grain structure. Smaller grains allow a better combination of ceramics, and this could slightly improve the connection in the case of the Vita VM13, although the difference in size between these two types of ceramics is insignificant.

In addition, the SEM morphological studies showed that after firing, the changes occurred in the concentration of elements at the ceramics-alloy border. The content of Zr, Ti and Ce decreased in individual ceramic layers. This proves the occurrence of diffusion in the studied areas as a result of diffusion processes. Probably the Si element diffused into the alloy area because its content increased, as compared to the composition before firing. As for Al, its quantity decreased. These processes led to the formation of an oxide layer, which significantly affects the strength and tightness of the joint.



Jeśli chodzi o Al to jego ilość się zmniejszyła. Procesy te prowadzą do powstania warstwy tlenkowej, która w istotny sposób wpływa pozytywnie na wytrzymałość i szczelność złącza.

Z aktualnych doniesień literaturowych wynika, że zastosowanie jonów na powierzchnię metalu oraz oksydacja powodują minimalny wzrost chropowatości. Występowanie metali nieszlachetnych prowadzi do znacznie niższych sił wiązania i nie wpływa pozytywnie na połączenie. Zauważa się korelację między chropowatością powierzchni, a siłą wiązania. Konieczne jest wykonanie mechanicznej obróbki strumieniowo- ścierniej poprzez zastosowanie  $Al_2O_3$ . Dowodzą tego również autorzy Susanne Enghardt, Gert Richter, Edgar Richter, Bernd Reitemeier, Michael H. Walter, publikacji pt. „Experimental Investigations on the Influence of Adhesive Oxides on the Metal-Ceramic Bond”. Autor innej publikacji również potwierdza, że wypiskowana powierzchnia wpływa na tworzenie się drobnych nieregularności, które polepszają połączenie poprzez wytworzenie tzw. mechanicznych „mikrozaczepów” [6-8].

## Wnioski

Warstwa opakerowa wpływa na połączenie stopu z ceramiką. Najlepsze rezultaty wykazuje gdy porowatość jest minimalna, a ziarna są małe. Warstwa ta nie może różnić się znacznie twardością od pozostałych warstw, gdyż będzie bardziej podatna na kruche pękanie. Duża różnica w module sprężystości pomiędzy stopem, a materiałem ceramicznym jest niewskazana.




Na podstawie wyników badań nie stwierdzono wpływu rodzaju opakera na wytrzymałość połączenia stopu z ceramiką.

Mniejsze ziarna proszku ceramicznego umożliwiają lepsze połączenie się ceramiki, a to mogło minimalnie polepszyć połączenie w przypadku próbki A, mimo że różnica w wielości między tymi ceramikami jest niewielka.

## Podziękowania

*Autorzy pragną podziękować mgr inż. Krzysztofowi Jakubowskiemu, który umożliwił przeprowadzenie badań. Praca powstała dzięki działalności statutowej.*

## ORCID iDs

Z. Kula:  <https://orcid.org/0000-0002-6899-9098>  
 Ł. Kołodziejczyk:  <https://orcid.org/0000-0002-4704-4188>  
 H. Szymanowski:  <https://orcid.org/0000-0002-4243-6342>

Current literature reports show that the use of ions on the metal surface and oxidation cause a minimal increase in roughness. The occurrence of base metals leads to significantly lower bonding forces and does not affect the connection positively. There is a correlation between the surface roughness and the bond strength. It is necessary to perform mechanical abrasive blasting by using  $Al_2O_3$ . This is also proved by the authors Susanne Enghardt, Gert Richter, Edgar Richter, Bernd Reitemeier, Michael H. Walter, in the publication entitled “Experimental Investigations on the Influence of Adhesive Oxides on the Metal-Ceramic Bond”. The author of another publication also confirms that the sandblasted surface affects the formation of small irregularities that improve the connection by creating so-called mechanical “micro-fasteners” [6-8].

## Conclusions

The opaque layer affects bonding of the alloy with the ceramics. The best results can be noticed when porosity is minimal and grains are small. However, in terms of hardness, this layer cannot differ much from the other ones, as it will be more prone to fracture. A large difference in the elastic moduli between the alloy and the ceramic material is not advisable.

Based on the study results, it was found that the type of the opaque had no effect on the strength of the ceramics-alloy connection.

Smaller grains of the ceramic powder allow better combination of ceramics, and this could improve the connection in the case of sample A even though the difference in plurality between these ceramics is small.

## Acknowledgements

*The authors would like to thank mgr inż. Krzysztof Jakubowski who made it possible to conduct research. The work was created thanks to the statutory activity.*

## References

- [1] Ciaputa T.: Podstawy wykonawstwa prac protetycznych, Elamed, Katowice 2009.
- [2] Rao S.: Comparison of Fracture Toughness of All-Ceramic and Metal-Ceramic Cement Retained Implant Crowns: An In Vitro Study. J Indian Prosthodont Soc 14(4) (2014) 408-414.
- [3] Henriques B.: Microstructure, hardness, corrosion, resistance and porcelain shear bond strength comparison between cast and hot Pressed CoCrMo alloy for metal-ceramic dental restorations. Journal of the Mechanical Behavior of Biomedical Materials 12 (2012) 83-92.
- [4] Craig R.G.: Materiały stomatologiczne, Urban & Partner, Wrocław 2008.
- [5] Enghardt S.: Experimental Investigations on the Influence of Adhesive Oxides on the Metal-Ceramic Bond. Metals 5 (2015) 119-130.
- [6] Hajduga M.: Charakter połączenia strukturalnego ceramika-metal cz. 1: Nowoczesny Technik Dentystyczny 3 (2009) 32-34.
- [7] Hajduga M.: Charakter połączenia strukturalnego ceramika-metal cz. 2: Nowoczesny Technik Dentystyczny 4 (2009) 40-42.
- [8] Hajduga M.: Charakter połączenia strukturalnego ceramika-metal cz. 3: Nowoczesny Technik Dentystyczny 5 (2009) 26-27.
- [9] Dejak B.: Materiały ceramiczne dla protetyki: Protetyka stomatologiczna 6 (2006) 95-123.
- [10] Fahrenholtz W.G. G E Hilmas: Oxidation of ultra-high temperature transition metal diboride ceramics: International Materials Reviews 57(1) (2012) 61-72.
- [11] Mackiewicz S.: Dyfraktometria rentgenowska w badaniach nieniszczących, Popów 2005..